Spacetime structure of static solutions in Gauss-Bonnet gravity: Charged case

Takashi Torii[1,2] and Hideki Maeda[2]

[1]*Graduate School of Science, Waseda University, Shinjuku-ku, Tokyo 169-8555, Japan*

[2]*Advanced Research Institute for Science and Engineering, Waseda University, Shinjuku-ku, Tokyo 169-8555, Japan*

(Received 14 April 2005; published 14 September 2005)

We have studied spacetime structures of static solutions in the n-dimensional Einstein-Gauss-Bonnet-Maxwell-Λ system. Especially we focus on effects of the Maxwell charge. We assume that the Gauss-Bonnet coefficient α is non-negative and $4\tilde{\alpha}/\ell^2 \leq 1$ in order to define the relevant vacuum state. Solutions have the $(n-2)$-dimensional Euclidean submanifold whose curvature is $k = 1$, 0, or -1. In Gauss-Bonnet gravity, solutions are classified into plus and minus branches. In the plus branch all solutions have the same asymptotic structure as those in general relativity with a negative cosmological constant. The charge affects a central region of a spacetime. A branch singularity appears at the finite radius $r = r_b > 0$ for any mass parameter. There the Kretschmann invariant behaves as $O((r-r_b)^{-3})$, which is much milder than the divergent behavior of the central singularity in general relativity $O(r^{-4(n-2)})$. In the $k = 1$ and 0 cases plus-branch solutions have no horizon. In the $k = -1$ case, the radius of a horizon is restricted as $r_h < \sqrt{2\tilde{\alpha}}$ ($r_h > \sqrt{2\tilde{\alpha}}$) in the plus (minus) branch. Some charged black hole solutions have no inner horizon in Gauss-Bonnet gravity. There are topological black hole solutions with zero and negative mass in the plus branch regardless of the sign of the cosmological constant. Although there is a maximum mass for black hole solutions in the plus branch for $k = -1$ in the neutral case, no such maximum exists in the charged case. The solutions in the plus branch with $k = -1$ and $n \geq 6$ have an inner black hole and inner and outer black hole horizons. In the $4\tilde{\alpha}/\ell^2 = 1$ case, only a positive mass solution is allowed, otherwise the metric function takes a complex value. Considering the evolution of black holes, we briefly discuss a classical discontinuous transition from one black hole spacetime to another.

DOI: 10.1103/PhysRevD.72.064007 PACS numbers: 04.50.+h, 04.65.+e, 04.70.−s

I. INTRODUCTION

Recently a large number of studies in the field of black hole physics have focused on the question of higher dimensions. One of the reasons for this is the fascinating new picture of our universe called the braneworld universe [1–3]. Because the fundamental scale could be about TeV in this scenario, these models suggest that the creation of tiny black holes in the upcoming linear hadron collider could be possible [4]. This would be strong evidence of extra dimensions.

Underlying the braneworld model is an underlying fundamental theory, superstring/M theory [5], which is the most promising candidate to produce a quantum theory of gravity. Although superstring/M theory has been highly elaborated, it is not enough to understand black hole physics in the string context. Hence at present to take string effects perturbatively into classical gravity is one approach to the study of quantum gravity effects. With the restriction that the tension of a string be large as compared to the energy scale of other variables, i.e., in the α' expansion, where α' is the inverse string tension, the Gauss-Bonnet terms appear as the first curvature correction term to general relativity [6]. These are ghost-free combinations [7] and have quasilinear properties [8].

Against this background we studied spacetime structures of static solutions in the n-dimensional Einstein-Gauss-Bonnet-Λ system systematically [9]. The black hole solutions in Gauss-Bonnet gravity were first discovered by Boulware and Deser [10] and Wheeler [11], independently. Since then many types of black solutions have been intensively studied [9,12]. Beyond the Gauss-Bonnet action which is the second order Lovelock action [13], the black hole solution in general Lovelock gravity is analyzed in Refs. [14–16] without providing the explicit form of solution. These solutions have a good many characteristic properties which cannot be seen for black hole solutions in general relativity. Let us briefly review the characteristic properties of the uncharged solutions in Gauss-Bonnet gravity. We assume that the Gauss-Bonnet coefficient α, which corresponds to α', is non-negative, and a cosmological constant is either positive, zero, or negative. The general solutions are classified into plus and minus branches. For the negative mass parameter, a new type of singularity called a branch singularity appears at the nonzero finite radius $r = r_b > 0$. The divergent behavior around the singularity in Gauss-Bonnet gravity is milder than that around the central singularity in general relativity. A black hole solution with zero or negative mass exists in the plus branch even for a zero or positive cosmological constant. There is also an extreme black hole solution with positive mass, in spite of the lack of an electromagnetic charge.

In this paper we extend the previous investigations by including the Maxwell charge. In general relativity, the Maxwell charge affects the structure of the singularity, the number of horizons, and the thermodynamical proper-

ties. In general relativity, if we add the charge to a Schwarzschild black hole, an inner horizon appears, and the singularity becomes timelike so that a spacetime represents the Reissner-Nordström (RN) black hole. Since the singularity is timelike, a test observer can see it. This example seems to counter the cosmic censorship hypothesis (CCH), proposed by Penrose [17,18]. The CCH asserts that the singularities formed in the generic gravitational collapse of physical matter should be covered by the event horizon and remain invisible. There are two versions of the CCH. One of them is the weak cosmic censorship hypothesis, which asserts that observers at infinity should not see singularities. The other is the strong one, which asserts that any observers should not see them, i.e., a spacetime is globally hyperbolic. Nevertheless, the RN solution should not be considered as a counterexample to the strong version of the CCH. Penrose demonstrated that perturbations originating outside the black hole would be blueshifted infinitely at the inner horizon and that the inner horizon suffers from blue-sheet instability [19]. After a large number of analyses, it has been clarified that this type of inner horizon is unstable against the perturbations and transforms into a null, weak scalar curvature singularity [20,21]. The general proof of the CCH is, however, far from complete, and many counterexample candidates have been proposed in the framework of general relativity [22]. Then the following question arises: Can the string corrections support a system sufficiently for the CCH to hold? Furthermore, the charge may play an important role in the braneworld and anti-de Sitter/conformal field theory (adS/CFT) correspondence [23]. In fact, in the braneworld model in general relativity, a cosmological constant may be self-tuned to solve the cosmological constant problem in charged bulk spacetime [24]. From these points of view, investigations of the charged solution are important.

In Sec. II, we introduce our model and show solutions which are generalizations of the originals of Boulware and Deser's. In Sec. III, we review the charged solutions in general relativity for comparison. In Sec. IV, the general properties of the solutions in the Einstein-Gauss-Bonnet-Maxwell-Λ system with $4\tilde{\alpha}/\ell^2 < 1$, whose meaning is given in the text, are investigated. In Sec. V, we show $\tilde{M}$-r diagrams and study the number of horizons in each solution. The global structures of all solutions are summarized in the tables. Section VI is devoted to the analysis of the special case where $4\tilde{\alpha}/\ell^2 = 1$. In Sec. VII, we present conclusions and discuss related issues. Throughout this paper we use units such that $c = \hbar = k_B = 1$. As for notation and conversion we follow Ref. [25]. The Greek indices run $\mu, \nu = 0, 1, \ldots, n-1$.

II. MODEL AND SOLUTIONS

We start with the following n-dimensional ($n \geq 4$) action

$$S = \int d^n x \sqrt{-g}\left[\frac{1}{2\kappa_n^2}(R - 2\Lambda + \alpha L_{\rm GB})\right] + S_{\rm matter}, \quad (1)$$

where R and Λ are the n-dimensional Ricci scalar and the cosmological constant, respectively. $\kappa_n := \sqrt{8\pi G_n}$, where G_n is the n-dimensional gravitational constant. The Gauss-Bonnet Lagrangian $L_{\rm GB}$ is the combination of the Ricci scalar, the Ricci tensor $R_{\mu\nu}$, and the Riemann tensor $R_{\mu\nu\rho\sigma}$ as

$$L_{\rm GB} = R^2 - 4R_{\mu\nu}R^{\mu\nu} + R_{\mu\nu\rho\sigma}R^{\mu\nu\rho\sigma}. \quad (2)$$

In the four-dimensional case, the Gauss-Bonnet terms do not appear in the equation of motion but contribute merely as surface terms. α is the coupling constant of the Gauss-Bonnet terms. This type of action is derived from superstring theory in the low-energy limit [6]. In that case α is regarded as the inverse string tension and positive definite. For the stability of Minkowski spacetime, we consider only the case with $\alpha \geq 0$ in this paper. We consider the Maxwell gauge field as a matter field, whose action is

$$S_{\rm matter} = -\frac{1}{4\pi g_c^2}\int d^n x \sqrt{-g} F_{\mu\nu}F^{\mu\nu}, \quad (3)$$

where g_c is the Maxwell coupling constant.

The gravitational equation of the action (1) is

$$G_{\mu\nu} + \alpha H_{\mu\nu} + \Lambda g_{\mu\nu} = \kappa_n^2 T_{\mu\nu}, \quad (4)$$

where

$$G_{\mu\nu} := R_{\mu\nu} - \frac{1}{2}g_{\mu\nu}R, \quad (5)$$

$$H_{\mu\nu} := 2[RR_{\mu\nu} - 2R_{\mu\alpha}R^{\alpha}{}_{\nu} - 2R^{\alpha\beta}R_{\mu\alpha\nu\beta} + R_{\mu}^{\alpha\beta\gamma}R_{\nu\alpha\beta\gamma}] - \frac{1}{2}g_{\mu\nu}L_{\rm GB}. \quad (6)$$

The energy-momentum tensor of the Maxwell field is

$$T_{\mu\nu} = \frac{1}{4\pi g_c^2}\left(F_{\mu\alpha}F_{\nu}{}^{\alpha} - \frac{1}{4}g_{\mu\nu}F_{\alpha\beta}F^{\alpha\beta}\right). \quad (7)$$

The Maxwell equation is obtained as

$$\nabla_\alpha F^{\alpha\mu} = 0. \quad (8)$$

We assume static spacetime and adopt the following line element:

$$ds^2 = -f(r)e^{-2\delta(r)}dt^2 + f^{-1}(r)dr^2 + r^2 d\Omega_{n-2}^2, \quad (9)$$

where $d\Omega_{n-2}^2 = \gamma_{ij}dx^i dx^j$ is the metric of the $(n-2)$-dimensional Einstein space.

The gravitational Eq. (4) provides $\delta \equiv 0$ without loss of generality. The Maxwell equation is written by using the electric field $E(r)$ defined by $E(r) := F_{rt}$ as

$$\frac{d}{dr}(r^{n-2}E) = 0. \quad (10)$$

Here we do not consider the magnetic field. This equation is integrated to give

$$E = \frac{Q}{r^{n-2}}, \tag{11}$$

where the integration constant Q is the electric charge.

The equation of the metric function f is then written as

$$\begin{aligned} & rf' - (n-3)(k-f) - \frac{n-1}{\ell^2} r^2 \\ & \quad + \frac{\tilde{\alpha}}{r^2}(k-f)[2rf' - (n-5)(k-f)] \\ & \quad = -\frac{\kappa_n^2 Q^2}{4(n-2)(n-3)^2 \pi g_c^2 r^{2n-6}}, \end{aligned} \tag{12}$$

where $\tilde{\alpha} := (n-3)(n-4)\alpha$ and $\Lambda = -(n-1)\times(n-2)/(2\ell^2)$. Note that a negative (positive) Λ gives a positive (negative) ℓ^2. k is the curvature of the $(n-2)$-dimensional Einstein space and takes 1 (positive curvature), 0 (flat), or -1 (negative curvature). The general solution of Eq. (12) is obtained [26] as

$$f = k + \frac{r^2}{2\tilde{\alpha}} \left\{ 1 \mp \sqrt{1 + 4\tilde{\alpha}\left[\frac{\tilde{M}}{r^{n-1}} - \frac{1}{\ell^2} - \frac{(n-3)\tilde{Q}^2}{2r^{2(n-2)}} \right]} \right\}, \tag{13}$$

where

$$\tilde{M} := \frac{16\pi G_n M}{(n-2)\Sigma_{n-2}^k}, \tag{14}$$

$$\tilde{Q}^2 := \frac{\kappa_n^2 Q^2}{2(n-2)(n-3)^2 \pi g_c^2}. \tag{15}$$

The integration constant M is proportional to the mass of a black hole for the black hole spacetime. Σ_{n-2}^k is the volume of the unit $(n-2)$-dimensional Einstein space. There are two families of solutions which correspond to the sign in front of the square root in Eq. (13). We call the family which has a minus (plus) sign the minus- (plus-) branch solution. By introducing new variables as $r := r/\ell$, $\bar{M} := \tilde{M}/\ell^{n-3}$, $\bar{Q} := \tilde{Q}/\ell^{n-3}$, and $\bar{\alpha} := \tilde{\alpha}/\ell^2$, the curvature radius ℓ is scaled out when the cosmological constant is nonzero. In the $\Lambda = 0$ case the variables are scaled as $r := r/\sqrt{\tilde{\alpha}}$, $\bar{M} := \tilde{M}/\sqrt{\tilde{\alpha}}$, and $\bar{Q} := \tilde{Q}/\sqrt{\tilde{\alpha}}$.

The global structure of a spacetime is characterized by properties of the singularities, horizons, and infinities. As for the definition of horizons we follow Ref. [9]. The solutions in this paper are classified into two types by horizon existence. The first is a black hole solution which has a black hole horizon. A solution which does not have a black hole horizon but has a locally naked singularity is a globally naked solution.

Since there are many parameters in our solution, such as $\tilde{\alpha}$, ℓ^2 (or Λ), $\tilde{M}$, $\tilde{Q}$, k, and $\pm$ branches, the analysis should be performed systematically. In this paper we employ $\tilde{M}$-r diagrams, which are explained in Ref. [9].

III. STATIC SOLUTIONS IN THE EINSTEIN-MAXWELL-Λ SYSTEM

In Gauss-Bonnet gravity, two branches of the static solution appear. The minus-branch solution reduces to the solution in the Einstein-Maxwell-Λ system in the limit of $\alpha \to 0$. The metric function f becomes

$$f = k - \frac{\tilde{M}}{r^{n-3}} + \frac{(n-3)}{2}\frac{\tilde{Q}^2}{r^{2n-6}} + \frac{r^2}{\ell^2}. \tag{16}$$

On the other hand, f diverges for the plus-branch solution in this limit, and there is no counterpart in the Einstein-Maxwell-Λ system. Before proceeding to the case with the Gauss-Bonnet terms, we first summarize the spacetime structure of the static solutions described by Eq. (9) with $\delta \equiv 0$ and (16) in the Einstein-Maxwell-Λ system for comparison. The spacetime structure and stability of the n-dimensional black hole solutions are extensively studied in Ref. [27]. Being interested in the charged solution, we assume $\tilde{Q} \neq 0$ throughout this paper.

There is a singularity at the center ($r = 0$). The Kretschmann invariant behaves

$$\mathcal{I} := R_{\mu\nu\rho\sigma}R^{\mu\nu\rho\sigma} = O\left(\frac{\tilde{Q}^2}{r^{4n-8}}\right), \tag{17}$$

around the center. The metric function f is positive around the center by Eq. (16), and the tortoise coordinate defined by

$$r^* := \int^r f^{-1} dr, \tag{18}$$

is finite at the center. Hence the singularity is always timelike [Fig. 1(a)].

The structure of the infinity is the same as that of the neutral case [9] except for the solution with $\Lambda = k = \tilde{M} = 0$. For this solution the $\tilde{Q}^2$ term is dominant, and the conformal diagram of the infinity is the same as that of the Minkowski spacetime.

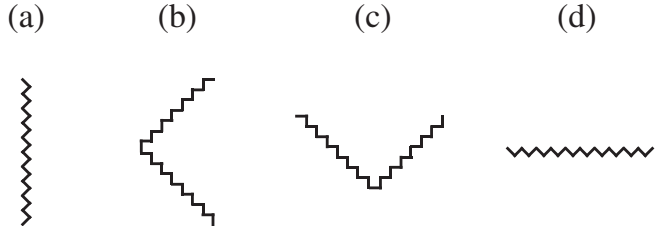

FIG. 1. The conformal diagrams around a singularity. Wavy lines denote singularities. There are time-reversed diagrams for (c) and (d).

The horizon plays an important role in determining the spacetime structure. The existence of the horizon is clearly visualized on the $\tilde{M}$-r diagram, especially in the case where there are many parameters. By Eq. (16), the $\tilde{M}$-r_h relation in the Einstein-Maxwell-Λ system is

$$\tilde{M} = r_h^{n-1}\left[\frac{1}{\ell^2} + \frac{(n-3)}{2}\frac{\tilde{Q}^2}{r_h^{2n-4}} + \frac{k}{r_h^2}\right]. \tag{19}$$

We consider here that the values of k, ℓ, and $\tilde{Q}$ are fixed so that this relation becomes a curve on the $\tilde{M}$-r diagram.

From the degeneracy condition of the horizon $f(r_{\rm ex}) = df/dr|_{r=r_{\rm ex}} = 0$, where $r_{\rm ex}$ is the radius of the degenerate horizon, we can show that the $\tilde{M}$-r_h curve on the diagram becomes vertical at this point. However, all the horizons at the vertical point are not necessarily degenerate. As shown in Ref. [9], if

$$\left.\frac{\partial \bar{f}}{\partial \tilde{M}}\right|_{r=r_h} = \infty, \tag{20}$$

where $\bar{f}(r, \tilde{M}) := f(r)$, the horizon at the vertical point can be nondegenerate. Although this condition (20) is satisfied only if $r_h \to 0$ limit in general relativity, we will find below that there is no such solution. Hence the horizon at any vertical point in the Einstein-Maxwell-Λ system is a degenerate horizon.

The mass $\tilde{M}$ and the charge $\tilde{Q}^2$ of the extreme solution are

$$\tilde{M} = \tilde{M}_{\rm ex} = 2r_{\rm ex}^{n-1}\left[\frac{(n-2)}{(n-3)\ell^2} + \frac{k}{r_{\rm ex}^2}\right], \tag{21}$$

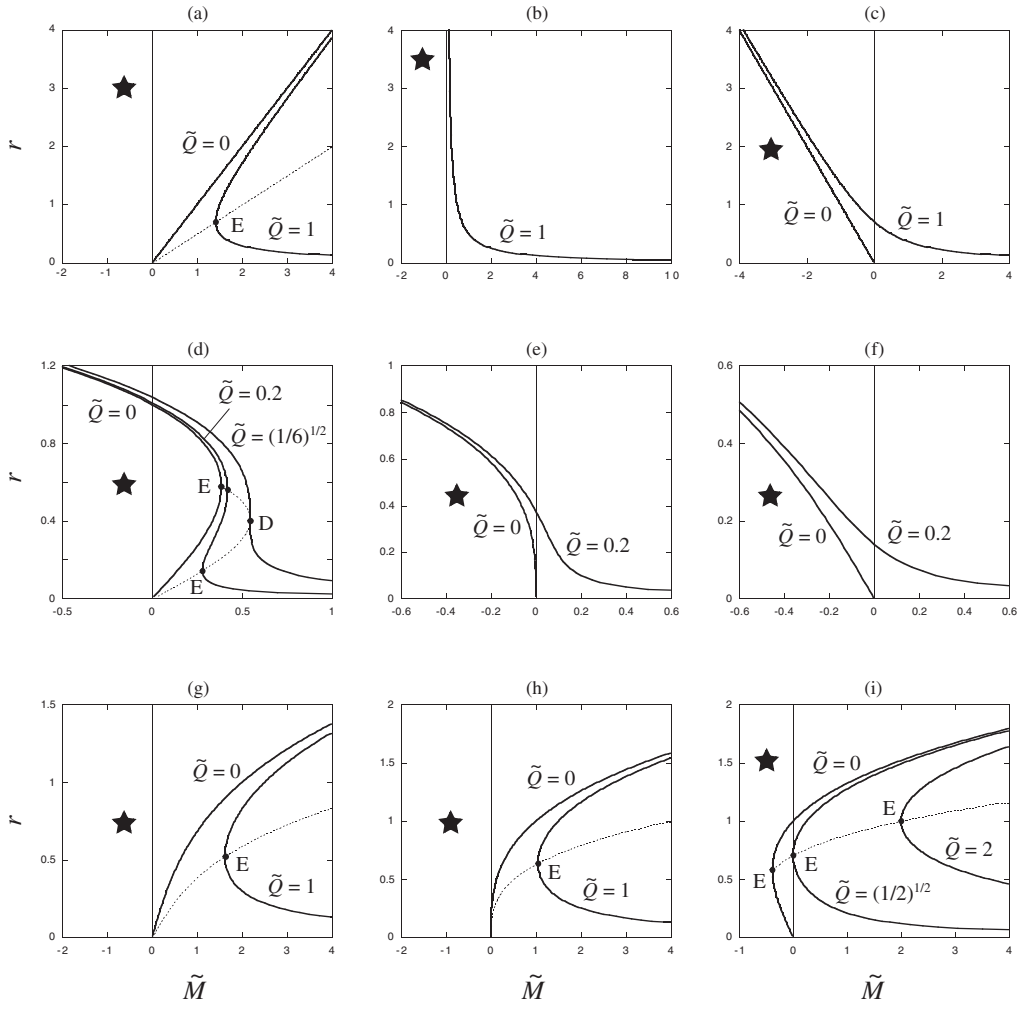

FIG. 2. The $\tilde{M}$-r diagrams for the static solutions in the four-dimensional Einstein-Maxwell-Λ system. The diagrams in the upper, middle, and lower rows are the $1/\ell^2 = 0$ (zero cosmological constant), $1/\ell^2 = -1$ (positive cosmological constant), and $1/\ell^2 = 1$ (negative cosmological constant) cases, respectively. The diagrams in the left, the middle, and the right columns are the $k = 1$, 0, and -1 cases, respectively. The $\tilde{M}$-r_h relations (thick curves) and the $\tilde{M}$-$r_{\rm ex}$ relations (dotted curves) are plotted. The dots with characters "E" and "D" imply the degenerate horizon and the doubly degenerate horizon, respectively. The region with a star which is bounded by the $\tilde{M}$-r_h curve represents an untrapped region. It changes from an untrapped region to a trapped region or vice versa by crossing the $\tilde{M}$-r_h curve. In cases with more than four dimensions, the $\tilde{M}$-r diagrams are qualitatively the same.

$$\tilde{Q}^2 = \tilde{Q}_{\rm ex}^2 = \frac{2r_{\rm ex}^{2(n-2)}}{(n-3)^2}\left[\frac{n-1}{\ell^2} + \frac{(n-3)k}{r_{\rm ex}^2}\right], \qquad (22)$$

respectively. By Eq. (22), there are extreme solutions only in the case where $\Lambda < 0$ and/or $k = 1$. On the $\tilde{M}$-r diagram the extreme solution is expressed by the point where two horizons coincide. When $d^2\tilde{M}/dr_h^2 = 0$ is satisfied at the finite radius $r_h = r_d$, the three horizons degenerate, and we call the horizon a doubly degenerate horizon.

We will examine a number of horizons of the solutions. The $\tilde{M}$-r diagrams are shown in Fig. 2, and the global structures are summarized in Tables I and II.

A. $\Lambda = 0$ case

By Eq. (19) we find

$$r_h^{n-3} = \frac{1}{2k}[\tilde{M} \pm \sqrt{\tilde{M}^2 - 2(n-3)k\tilde{Q}^2}] \qquad (23)$$

for $k \neq 0$, and

$$r_h^{n-3} = \frac{(n-3)\tilde{Q}^2}{2\tilde{M}} \qquad (24)$$

for $k = 0$.

In the $k = 1$ case, the solution is the n-dimensional RN solution [28]. The $\tilde{M}$-r diagram is shown in Fig. 2(a). For $\tilde{M} < \tilde{M}_{\rm ex}$, where $\tilde{M}_{\rm ex} = 2r_{\rm ex}^{n-3} = \sqrt{2(n-3)\tilde{Q}^2}$, the solution has no horizon and represents a spacetime with a globally naked singularity. For $\tilde{M} = \tilde{M}_{\rm ex}$ the solution is the n-dimensional extreme RN black hole solution. The term of the square root in Eq. (23) vanishes, and a degenerate horizon locates at $r_{\rm ex} = [(n-3)\tilde{Q}^2/2]^{1/2(n-3)}$. For $\tilde{M} > \tilde{M}_{\rm ex}$, the solution has black hole and inner horizons, which have radii with the plus and the minus signs in Eq. (23), respectively, and represents the RN black hole spacetime.

TABLE I. The classification of the spacetime structures of the static solutions in the Einstein-Maxwell-Λ system. The numbers in the column "Type" imply the types of the conformal diagrams in Figs. 6–9. For the $\Lambda > 0$ and $k = 1$ case, see Table II.

k	$\Lambda = 0$		$\Lambda > 0$		$\Lambda < 0$	
	$\tilde{M}$	Type	$\tilde{M}$	Type	$\tilde{M}$	Type
1	$\tilde{M} < \tilde{M}_{\rm ex}$	sI	see Table II		$\tilde{M} < \tilde{M}_{\rm ex}$	sIV
	$\tilde{M} = \tilde{M}_{\rm ex}$	dbI			$\tilde{M} = \tilde{M}_{\rm ex}$	dbII
	$\tilde{M} > \tilde{M}_{\rm ex}$	bVII			$\tilde{M} > \tilde{M}_{\rm ex}$	bIV
0	$\tilde{M} \leq 0$	sI	any	sII	$\tilde{M} < \tilde{M}_{\rm ex}$	sIV
	$\tilde{M} > 0$	sIII			$\tilde{M} = \tilde{M}_{\rm ex}$	dbII
					$\tilde{M} > \tilde{M}_{\rm ex}$	bIV
-1	any	sIII	any	sII	$\tilde{M} < \tilde{M}_{\rm ex}$	sIV
					$\tilde{M} = \tilde{M}_{\rm ex}$	dbII
					$\tilde{M} > \tilde{M}_{\rm ex}$	bIV

TABLE II. The classification of the spacetime structures of the static solutions in the $\Lambda > 0$ and $k = 1$ cases in the Einstein-Maxwell-Λ system. This table also shows the classification of the spacetime structures of the static solutions in the minus branch in the Einstein-Gauss-Bonnet-Maxwell-Λ system with $4\tilde{\alpha}/\ell^2 \neq 1$. In the latter case the mass of the extreme solutions is $\tilde{M}_{\rm ex}^{(i)} \to \tilde{M}_{\rm ex}^{(i-)}$, where $i = 1, 2$. The numbers in the column "Type" imply the types of the conformal diagrams in Figs. 6–9.

$\lvert\tilde{Q}\rvert < \lvert\tilde{Q}_d\rvert$		$\lvert\tilde{Q}\rvert = \lvert\tilde{Q}_d\rvert$		$\lvert\tilde{Q}\rvert > \lvert\tilde{Q}_d\rvert$	
$\tilde{M}$	Type	$\tilde{M}$	Type	$\tilde{M}$	Type
$\tilde{M} < \tilde{M}_{\rm ex}^{(1)}$	sII	$\tilde{M} < \tilde{M}_d$	sII	any	sII
$\tilde{M} = \tilde{M}_{\rm ex}^{(1)}$	dbIII	$\tilde{M} = \tilde{M}_d$	dsIII		
$\tilde{M}_{\rm ex}^{(1)} < \tilde{M} < \tilde{M}_{\rm ex}^{(2)}$	bVIII	$\tilde{M} > \tilde{M}_d$	sII		
$\tilde{M} = \tilde{M}_{\rm ex}^{(2)}$	dsII				
$\tilde{M} > \tilde{M}_{\rm ex}^{(2)}$	sII				

In the $k = 0$ case, the $\tilde{M}$-r_h diagram is shown in Fig. 2(b). For $\tilde{M} \leq 0$ the solution has no horizon and represents a spacetime with a globally naked singularity. For $\tilde{M} > 0$ the solution has a cosmological horizon and represents a spacetime with a globally naked singularity.

In the $k = -1$ case, the $\tilde{M}$-r_h diagram is shown in Fig. 2(c). The solution has a cosmological horizon for any value of $\tilde{M}$ and represents a spacetime with a globally naked singularity.

B. $\Lambda > 0$ case

In the $k = 1$ case, the solution is the n-dimensional RN-dS solution and has three horizons at most. The $\tilde{M}$-r_h diagram is shown in Fig. 2(d).

When the charge of the solution satisfies $0 < |\tilde{Q}| < |\tilde{Q}_d|$, there are two vertical points in the M-r_h diagram. Here $\tilde{Q}_d$ is the charge of the solution with a doubly degenerate horizon

$$\tilde{Q}_d^2 = \frac{2}{(n-2)(n-3)} r_d^{2(n-3)}, \qquad (25)$$

$$r_d^2 = \frac{(n-3)^2|\ell^2|}{(n-1)(n-2)}. \qquad (26)$$

These vertical point E's in Fig. 2(d) correspond to two degenerate horizons with radii $r_{\rm ex}^{(1)}$ and $r_{\rm ex}^{(2)}$ ($r_{\rm ex}^{(1)} < r_{\rm ex}^{(2)}$) calculated by solving Eq. (22) with respect to $r_{\rm ex}$, respectively. The former is realized by the degeneracy of the black hole and the inner horizons, while the latter is realized by the degeneracy of the black hole and the cosmological horizons. We denote the mass of these solutions by $\tilde{M}_{\rm ex}^{(1)}$ and $\tilde{M}_{\rm ex}^{(2)}$ ($\tilde{M}_{\rm ex}^{(1)} < \tilde{M}_{\rm ex}^{(2)}$), respectively. For $\tilde{M} < \tilde{M}_{\rm ex}^{(1)}$, the solution has a cosmological horizon and represents a spacetime with a globally naked singularity. For $\tilde{M} = \tilde{M}_{\rm ex}^{(1)}$, the solution has a degenerate black hole horizon and a cosmological horizon and represents the

extreme RN-dS black hole spacetime. For $\tilde{M}^{(1)}_{\rm ex} < \tilde{M} < \tilde{M}^{(2)}_{\rm ex}$, the solution has inner, black hole, and cosmological horizons. The spacetime is the RN-dS black hole spacetime. For $\tilde{M} = \tilde{M}^{(2)}_{\rm ex}$, the solution has inner and degenerate horizons. For $\tilde{M} > \tilde{M}^{(2)}_{\rm ex}$, the solution has a cosmological horizon and represents the spacetime with a globally naked singularity.

When $|\tilde{Q}| = |\tilde{Q}_d|$, there is a solution with a doubly degenerate horizon whose mass parameter is

$$\tilde{M} = \tilde{M}_d = \frac{4}{n-1} r_d^{n-3}. \tag{27}$$

The doubly degenerate horizon locates at $r = r_d$. This solution represents a spacetime with a globally naked singularity. The ratio of the charge to the mass is

$$\frac{|\tilde{Q}_d|}{\tilde{M}_d} = \sqrt{\frac{(n-1)^2}{8(n-2)(n-3)}}. \tag{28}$$

The ratio takes the largest value $|\tilde{Q}_d|/\tilde{M}_d = 3/4$ for $n = 4$. For $\tilde{M} \neq \tilde{M}_d$, the solution has a cosmological horizon and represents the spacetime with a globally naked singularity.

When $|\tilde{Q}| > |\tilde{Q}_d|$, any solution has a cosmological horizon and represents the spacetime with a globally naked singularity.

In the $k = 0$ and the $k = -1$ cases, the $\tilde{M}$-r diagrams are shown in Figs. 2(e) and 2(f), respectively. They have qualitatively similar structures. The solutions have one cosmological horizon for any value of $\tilde{M}$ and represent the spacetime with a globally naked singularity.

C. $\Lambda < 0$ case

The system with a negative cosmological constant has been intensively studied in the adS/CFT and braneworld contexts. Furthermore there are topological black hole solutions [29,30].

In the $k = 1$ case, the solution is the RN-adS solution. The $\tilde{M}$-r diagram is shown in Fig. 2(g). The $\tilde{M}$-r diagram in the $k = 0$ case is shown in Fig. 2(h). We can see that they have similar structures. There is one vertical point in the $\tilde{M}$-r_h diagrams. It corresponds to the degenerate horizon, whose solution has the mass and the charge calculated by Eqs. (21) and (22). The mass of both extreme solutions is positive. For $\tilde{M} < \tilde{M}_{\rm ex}$, the solution has no horizon and represents the spacetime with a globally naked singularity. For $\tilde{M} = \tilde{M}_{\rm ex}$, the solution has a degenerate black hole horizon and represents the extreme black hole spacetime. For $\tilde{M} > \tilde{M}_{\rm ex}$, the solutions have inner and black hole horizons. The solution with $k = 1$ represents the n-dimensional RN-adS black hole spacetime.

In the $k = -1$ case, the $\tilde{M}$-r diagram is shown in Fig. 2(i). The solutions are classified into three types. For $\tilde{M} < \tilde{M}_{\rm ex}$, the solution has no horizons and represents the spacetime with a globally naked singularity. For $\tilde{M} = \tilde{M}_{\rm ex}$, the solution has a degenerate black hole horizon and represents the extreme black hole spacetime. For $\tilde{M} > \tilde{M}_{\rm ex}$, the solution has inner and black hole horizons and represents the black hole spacetime. Because of the first term on the right-hand side (rhs) of Eq. (19), a black hole solution with zero or negative mass can exist. As seen from Fig. 2(i), the black hole solution with the lightest mass for a fixed charge is the extreme solution. When the charge is small, the extreme black hole solution has negative mass. When $|\tilde{Q}| = |\tilde{Q}_{\rm ex,0}|$, where

$$\tilde{Q}^2_{\rm ex,0} := \frac{2}{(n-2)(n-3)} \left(\frac{n-3}{n-2}\ell^2\right)^{n-3}, \tag{29}$$

the extreme black hole solution has zero mass, and its horizon radius is

$$r_{\rm ex} = \sqrt{\frac{n-3}{n-2}}\ell. \tag{30}$$

For the charge $|\tilde{Q}| > |\tilde{Q}_{\rm ex,0}|$, all the black hole solutions have positive mass.

IV. GENERAL PROPERTIES OF SOLUTIONS IN THE EINSTEIN-GAUSS-BONNET-MAXWELL-Λ SYSTEM

We proceed to the cases with Gauss-Bonnet terms. First, let us discuss the general properties of the static solutions in this system.

For the well-defined theory with the relevant vacuum state ($\tilde{M} = \tilde{Q} = 0$), we assume

$$\frac{4\tilde{\alpha}}{\ell^2} \leq 1. \tag{31}$$

In this and the next sections, we study the $4\tilde{\alpha}/\ell^2 < 1$ case. The special case of $4\tilde{\alpha}/\ell^2 = 1$ will be investigated in Sec. VI.

The square of the effective curvature radius is defined by [9]

$$\ell^2_{\rm eff} := \frac{\ell^2}{2}\left(1 \pm \sqrt{1 - \frac{4\tilde{\alpha}}{\ell^2}}\right). \tag{32}$$

In Sec. III, we showed the structures of the infinity of the solutions, which depend on the value of ℓ^2, in general relativity. By replacing ℓ^2 in the discussion in general relativity by $\ell^2_{\rm eff}$ the structures of the infinity in the Einstein-Gauss-Bonnet-Maxwell-Λ system are obtained.

In general relativity there is a central singularity for any charged solution. In Gauss-Bonnet gravity the inside of the square root of Eq. (13) vanishes at the finite radius $r = r_b$, and the other type of singularity, called the branch singularity, appears there. The $\tilde{M}$-r_b relation becomes

$$\tilde{M} = \tilde{M}_b := -\left(1 - \frac{4\tilde{\alpha}}{\ell^2}\right)\frac{r_b^{n-1}}{4\tilde{\alpha}} + \frac{(n-3)\tilde{Q}^2}{2r_b^{n-3}}. \tag{33}$$

This relation is independent of k. In the neutral case $\tilde{Q} = 0$, the branch singularity appears only for the solution with negative mass [9], while all the solutions have branch singularity in the charged case. Around the branch singularity the Kretschmann invariant behaves as

$$\mathcal{I} \sim O[(r - r_b)^{-3}]. \tag{34}$$

From the condition (31), r_b decreases monotonically as $\tilde{M}$ increases and asymptotically approaches zero in the limit of $\tilde{M} \to \infty$. It is noted that the divergent behavior of the branch singularity is milder than that of the central singularity in general relativity [see Eqs. (17) and (34)].

The metric function f behaves around the branch singularity as

$$f(r) \approx \left(k + \frac{r_b^2}{2\tilde{\alpha}}\right) \mp \frac{r_b^2}{2\tilde{\alpha}} \times \sqrt{\frac{n-1}{r_b}\left(1 - \frac{4\tilde{\alpha}}{\ell^2}\right) + \frac{2(n-3)^2\tilde{\alpha}\tilde{Q}^2}{r_b^{2n-3}}}(r - r_b)^{1/2}. \tag{35}$$

Hence when $k = 1$ or 0, the singularity is timelike [Fig. 1(a)]. When $k = -1$, the singularities are timelike and spacelike [Fig. 1(d)] for $r_b > \sqrt{2\tilde{\alpha}}$ and $r_b < \sqrt{2\tilde{\alpha}}$, respectively. In the special case of $k = -1$ and $r_b = \sqrt{2\tilde{\alpha}}$, the singularities are spacelike and timelike for the minus and plus branches, respectively.

On the horizon the metric function f vanishes: $f(r_h) = 0$, and we find

$$\pm\left(1 + \frac{2\tilde{\alpha}k}{r_h^2}\right) = \sqrt{1 + 4\tilde{\alpha}\left[\frac{\tilde{M}}{r_h^{n-1}} - \frac{1}{\ell^2} - \frac{(n-3)\tilde{Q}^2}{2r_h^{2(n-2)}}\right]} > 0, \tag{36}$$

where the signs on the left-hand side (lhs) represent the minus/plus branches. Hence

$$r_h^2 < -2\tilde{\alpha}k \qquad \text{(for the plus branch)}, \tag{37}$$

$$r_h^2 > -2\tilde{\alpha}k \qquad \text{(for the minus branch)}. \tag{38}$$

By these conditions it is concluded that there is no horizon for $k = 1, 0$ in the plus branch. When $k = -1$, the horizon radius is restricted as $r_h < \sqrt{2\tilde{\alpha}}$ ($r_h > \sqrt{2\tilde{\alpha}}$) in the plus (minus) branch.

The $\tilde{M}$-r_h relation is

$$\tilde{M} = r_h^{n-1}\left[\frac{1}{\ell^2} + \frac{(n-3)}{2}\frac{\tilde{Q}^2}{r_h^{2n-4}} + \frac{k}{r_h^2}\left(1 + \frac{\tilde{\alpha}k}{r_h^2}\right)\right]. \tag{39}$$

For $k = 0$ this relation is the same as that in general relativity (19). For $k = -1$ the solution with $r_h = \sqrt{2\tilde{\alpha}}$ has a branch singularity at $r = r_B := \sqrt{2\tilde{\alpha}}$ where

$$\tilde{M} = \tilde{M}_B := \frac{(2\alpha)^{(n-3)/2}}{2}\left[-\left(1 - \frac{4\tilde{\alpha}}{\ell^2}\right) + \frac{(n-3)\tilde{Q}^2}{(2\tilde{\alpha})^{n-3}}\right]. \tag{40}$$

This implies that the sequence of solutions is divided by the branch singularity into the plus and the minus branches in the $k = -1$ case. It is seen that the $\tilde{M}$-r_h curve in the $\tilde{M}$-r diagram terminates at the $\tilde{M}$-r_b curve just at the point we call the branch point (point B in Figs. 3 and 4). For the mass parameter with $\tilde{M} \neq \tilde{M}_B$, the horizon radius is always larger than r_b. While $\tilde{M}_B$ is always negative in the neutral case, $\tilde{M}_B$ can be zero in the charged case by tuning the charge $\tilde{Q}$ as

$$\tilde{Q}^2 = \tilde{Q}_{B,0}^2 := \frac{1}{n-3}\left(1 - \frac{4\tilde{\alpha}}{\ell^2}\right)(2\tilde{\alpha})^{n-3}. \tag{41}$$

For $|\tilde{Q}| < |\tilde{Q}_{B,0}|$ ($|\tilde{Q}| > |\tilde{Q}_{B,0}|$), $\tilde{M}_B$ is negative (positive).

As we will see in the next section, in the $\tilde{M}$-r diagram of the $\tilde{M}$-r_h curve there are some vertical points. In Gauss-Bonnet gravity,

$$\left.\frac{\partial \bar{f}}{\partial \tilde{M}}\right|_{r=r_h} = \mp\frac{1}{r_h^{n-3}}\left\{1 + 4\tilde{\alpha}\left[\frac{\tilde{M}}{r_h^{n-1}} - \frac{1}{\ell^2} - \frac{(n-3)\tilde{Q}^2}{2r_h^{2(n-2)}}\right]\right\}^{-1/2} \tag{42}$$

is finite, so that the horizons at the vertical points are degenerate except for $r_h \to r_b$, where the condition (20) is satisfied. However, the $\tilde{M}$-r_h curve is tangent to the $\tilde{M}$-r_b curve at the branch point, and the $\tilde{M}$-r_b curve monotonically decreases. Thus the $\tilde{M}$-r_h curve cannot be vertical at the branch point. As a result the horizons at all the vertical points are degenerate (for this analysis, see Ref. [9].)

In the extreme cases, the relations between the mass, the charge, and the horizon radius are written as

$$\tilde{M} = \tilde{M}_{\rm ex} = 2r_{\rm ex}^{n-1}\left[\frac{(n-2)}{(n-3)\ell^2} + \frac{k}{r_{\rm ex}^2} + \frac{(n-4)\tilde{\alpha}k^2}{(n-3)r_{\rm ex}^4}\right], \tag{43}$$

$$\tilde{Q}^2 = \tilde{Q}_{\rm ex}^2 = \frac{2r_{\rm ex}^{2(n-2)}}{(n-3)^2}\left[\frac{n-1}{\ell^2} + \frac{(n-3)k}{r_{\rm ex}^2} + \frac{(n-5)\tilde{\alpha}k^2}{r_{\rm ex}^4}\right]. \tag{44}$$

In five dimensions the last term in Eq. (44) vanishes, and the charge of the extreme solution has the same expression as that in general relativity. This implies that degenerate horizons appear at the same radius as those appearing in general relativity if we choose the same charge value. However, the mass of the extreme solution is different from that in general relativity. Equation (44) is rewritten as

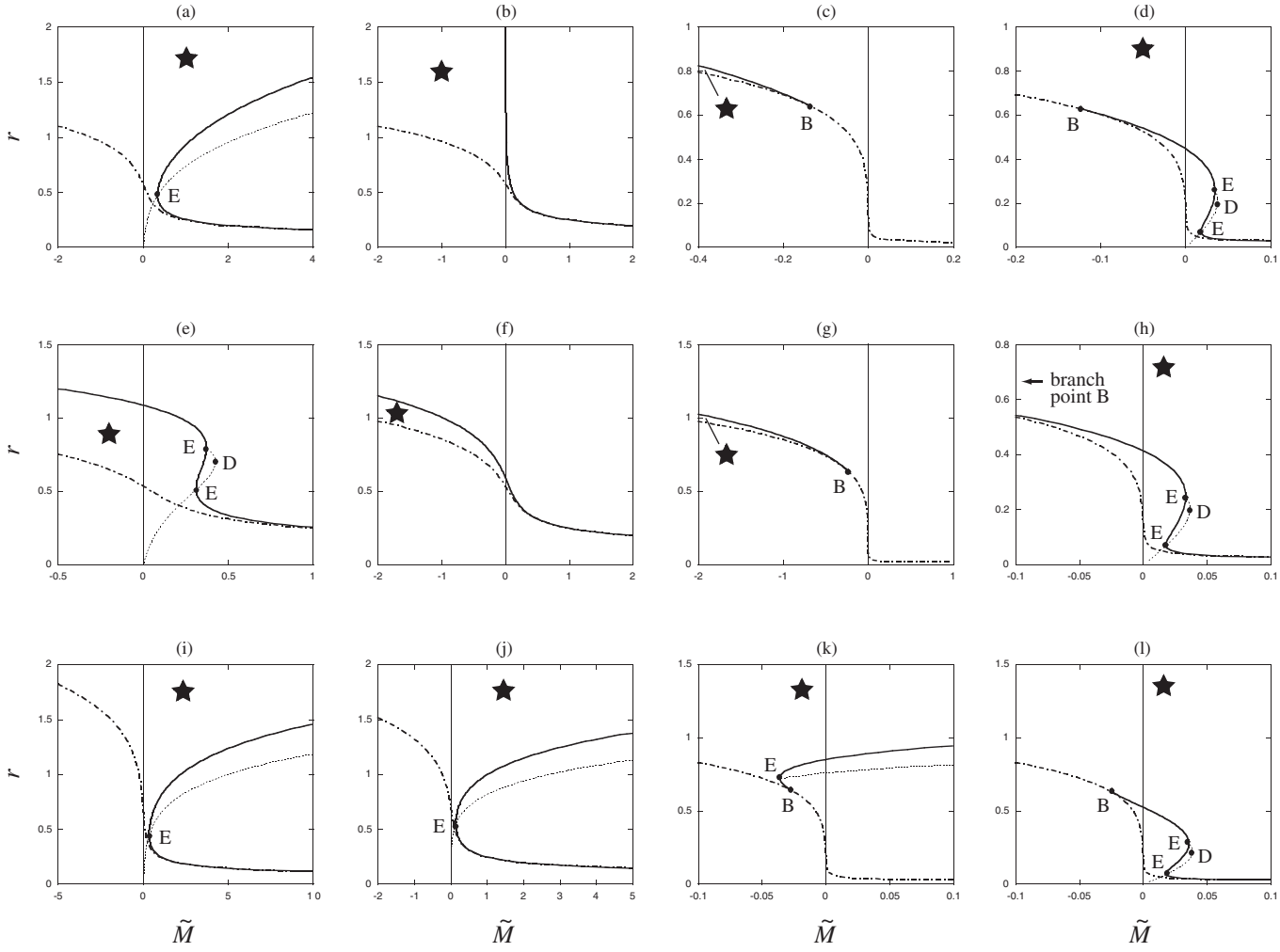

FIG. 3. The $\tilde{M}$-r diagrams of the static solutions in the six-dimensional Einstein-Gauss-Bonnet-Maxwell-Λ system with $4\tilde{\alpha}/\ell^2 \neq 1$. The diagrams in the upper, middle, and lower rows are the $1/\ell^2 = 0$ (zero cosmological constant), $1/\ell^2 = -1$ (positive cosmological constant), and $1/\ell^2 = 1$ (negative cosmological constant) cases, respectively. The diagrams in the columns from the left-hand side are the $k = 1$ (the minus branch), 0 (the minus branch), -1 (the minus branch), and -1 (the plus branch) cases, respectively. We show the $\tilde{M}$-r_h relations (thick solid curves) and the $\tilde{M}$-r_b relations (dot-dashed curves). We set $\tilde{\alpha} = 0.2$ and $\tilde{Q} = 0.1$ ($k = 1, 0$) and $\tilde{Q} = 10^{-3}$ ($k = -1$). We choose the value of the charge as $|\tilde{Q}| < |\tilde{Q}_d|$ in the $k = -1$ case. Otherwise, the two extreme solutions in the plus branch coincide, and the $\tilde{M}$-r_h relation becomes single valued. The dotted curve represents a sequence of the degenerate horizon ($\tilde{M}$-$r_{\rm ex}$ relations) by varying $\tilde{Q}$. Below the $\tilde{M}$-r_b line, there are no solutions. The dots labeled "E," "D," and "B" imply the degenerate horizon, the doubly degenerate horizon, and the branch point, respectively. See Fig. 2 for the meanings of the stars. The $\tilde{M}$-r diagrams of the higher-dimensional solutions with $n \geq 6$ have similar configurations to these.

$$U(r_{\rm ex}) := \frac{n-1}{\ell^2} r_{\rm ex}^{2n-4} + (n-3)k r_{\rm ex}^{2n-6} + \tilde{\alpha} k^2 (n-5) r_{\rm ex}^{2n-8} = \frac{(n-3)^2}{2} \tilde{Q}^2. \tag{45}$$

The function $U(r_{\rm ex})$ is defined in the range $r_{\rm ex} \geq 0$. If $U(r_{\rm ex})$ is negative semidefinite, there is no extreme solution. If $U(r_{\rm ex})$ is a monotonically increasing function from zero to infinity, there is a certain mass $\tilde{M}_{\rm ex}$ where the solution becomes extreme for any value of $\tilde{Q}$. We denote the mass of the extreme solution in the plus (minus) branch as $\tilde{M}_{\rm ex}^{(+)}$ ($\tilde{M}_{\rm ex}^{(-)}$). When more than one extreme solution exists in the same branch, we denote their mass as $\tilde{M}_{\rm ex}^{(1+)}$, $\tilde{M}_{\rm ex}^{(2+)}, \ldots$ ($\tilde{M}_{\rm ex}^{(1-)}, \tilde{M}_{\rm ex}^{(2-)}, \ldots$).

If $U(r_{\rm ex})$ is not a monotonic function, there are extremal points, which correspond to the solutions with a doubly degenerate horizon. We should take care not to confuse these extremal points of the function $U(_{\rm ex})$ with the extremal solution with degenerate horizons.

Although there may be a horizon with more degeneracy in general, in the present system up to a doubly degenerate horizon can appear. Hence examining the extremal points of $U(r_{\rm ex})$, we find the condition and location of the doubly degenerate horizon $r = r_d$ such that $dU/dr_{\rm ex}|_{r_{\rm ex}=r_d} = 0$. As the charge $\tilde{Q}$ is varied, the number of the roots $r_{\rm ex}$ in

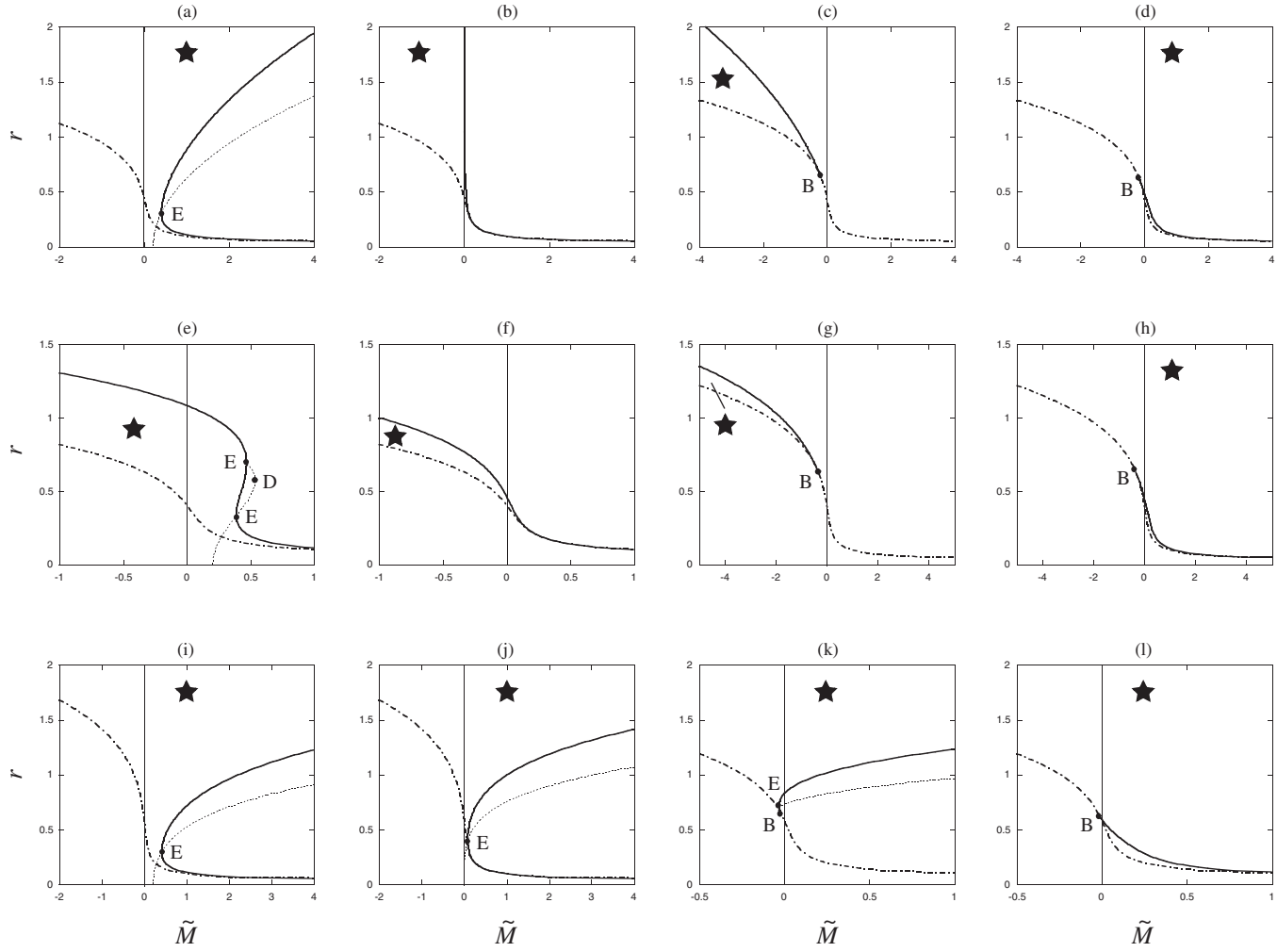

FIG. 4. The $\tilde{M}$-r diagrams of the static solutions in the five-dimensional Einstein-Gauss-Bonnet-Maxwell-Λ system with $4\tilde{\alpha}/\ell^2 \neq 1$. The diagrams in the upper, middle, and lower rows are the $1/\ell^2 = 0$ (zero cosmological constant), $1/\ell^2 = -1$ (positive cosmological constant), and $1/\ell^2 = 1$ (negative cosmological constant) cases, respectively. The diagrams in the columns from the left-hand side are the $k = 1$ (the minus branch), 0 (the minus branch), -1 (the minus branch), and -1 (the plus branch) cases, respectively. We show the $\tilde{M}$-r_h relations (thick lines) and the $\tilde{M}$-r_b relations (dot-dashed lines). We set $\tilde{\alpha} = 0.2$ and $\tilde{Q} = 0.1$. Below the $\tilde{M}$-r_b line, there are no solutions. The dotted curve represents a sequence of the degenerate horizon ($\tilde{M}$-$r_{\rm ex}$ relations) by varying $\tilde{Q}$. See Figs. 2 and 3 for the meanings of the dots and the stars.

Eq. (45) changes at the extremal points of the function $U(r_{\rm ex})$. When $\Lambda = 0$, the doubly degenerate horizon appears at

$$r_d^2 = -\frac{(n-4)(n-5)}{(n-3)^2} k\tilde{\alpha}. \tag{46}$$

Since the lhs of this equation is positive, k must be -1 and $n \geq 6$. Furthermore since $r_d < \sqrt{\tilde{\alpha}}$, the doubly degenerate horizon exists only in the plus branch. Then the mass and the charge of the solution are given by Eqs. (43) and (45) as

$$\tilde{M}_d = \frac{4}{n-5} r_d^{n-3}, \tag{47}$$

$$\tilde{Q}_d^2 := \frac{2}{(n-3)^2} U(r_d) = \frac{2}{(n-3)(n-4)} r_d^{2(n-3)}. \tag{48}$$

When $\Lambda \neq 0$, the doubly degenerate horizon appears at

$$r_d^2 = -\frac{(n-3)^2\ell^2 B}{2(n-1)(n-2)}, \tag{49}$$

and the mass and the charge of the solution become

$$\tilde{M}_d = 2r_d^{n-5}k^2\left[\frac{4(n-4)\tilde{\alpha}}{(n-1)(n-3)} - \frac{(n-3)^2\ell^2 B}{(n-1)^2(n-2)k}\right], \tag{50}$$

$$\tilde{Q}_d^2 = r_d^{2(n-4)} k^2 \left[\frac{4(n-5)\tilde{\alpha}}{(n-2)(n-3)^2} - \frac{(n-3)\ell^2 B}{(n-1)(n-2)^2 k} \right], \tag{51}$$

where

$$B := k \pm |k| \sqrt{1 - \frac{4\tilde{\alpha}(n-1)(n-2)(n-4)(n-5)}{(n-3)^4 \ell^2}}. \tag{52}$$

Note that the sign $\pm$ does not correspond to the signs of the solution branches but is determined to make the rhs of Eq. (49) positive. If both signs give negative $\ell^2 B$, there are two sets of parameters which give the solutions with a doubly degenerate horizon. When $|\tilde{Q}_d|$ is single valued (namely, there is only one value of the charge which gives a doubly degenerate horizon), two extreme solutions exist for $|\tilde{Q}| < |\tilde{Q}_d|$, while no extreme solution exists for $|\tilde{Q}| > |\tilde{Q}_d|$.

V. M-r_h DIAGRAM AND SPACETIME STRUCTURE

In the previous section, we discussed properties of the singularity, the infinity, and the horizons of the solutions in the Einstein-Gauss-Bonnet-Maxwell-Λ system. In this section we focus on the number of horizons and show the spacetime structures by taking into account the above properties. The 5-dimensional black hole solution in the present system is studied in Ref. [31] from the adS/CFT point of view, and the black hole solution without cosmological constant is analyzed recently in Ref. [32]. To clarify our considerations, the $\tilde{M}$-r diagrams are shown in Figs. 3 ($n = 6$) and 4 ($n = 5$). The spacetime structures of the solutions are summarized in Tables II, III, and IV.

A. $\Lambda = 0$

1. $k = 1$ case

The solution in the plus branch does not have a horizon and represents a spacetime with a globally naked singularity.

The $\tilde{M}$-r diagrams of the minus-branch solutions are shown in Figs. 3(a) ($n = 6$) and 4(a) ($n = 5$). Since the function $U(r_{\rm ex})$ monotonically increases from zero to infinity, there is an extreme solution for any $\tilde{Q}$. The extreme solution has the positive mass $\tilde{M}_{\rm ex}^{(-)} > 0$. For $\tilde{M} < \tilde{M}_{\rm ex}^{(-)}$, the solution has no horizon and represents a spacetime with a globally naked singularity. For $\tilde{M} = \tilde{M}_{\rm ex}^{(-)}$, the solution has a degenerate horizon and represents the extreme black hole spacetime. In the five-dimensional case, the mass and the horizon radius of the extreme black hole are $\tilde{M}_{\rm ex}^{(-)} = 2|\tilde{Q}| + \tilde{\alpha}$ and $r_{\rm ex} = \sqrt{|\tilde{Q}|}$, respectively. For $\tilde{M} > \tilde{M}_{\rm ex}^{(-)}$, the solution has inner and black hole horizons and represents the black hole spacetime.

2. $k = 0$ case

The solution in the plus branch does not have a horizon and represents a spacetime with a globally naked singularity.

The $\tilde{M}$-r diagrams of the minus-branch solutions are shown in Figs. 3(b) ($n = 6$) and 4(b) ($n = 5$). The $\tilde{M}$-r_h relation becomes $\tilde{M} = (n-3)\tilde{Q}^2/2r_h^{n-3}$, and the horizon radius diverges in the $\tilde{M} \to 0+$ limit. For $\tilde{M} \le 0$, the solution has no horizon and represents a spacetime with a

TABLE III. The classification of the spacetime structures of the static solutions in the Einstein-Gauss-Bonnet-Maxwell-Λ system with $4\tilde{\alpha}/\ell^2 \neq 1$. The numbers in the column "Type" imply the types of the conformal diagrams in Figs. 6–9. For the minus-branch solutions with $\Lambda > 0$ and $k = 1$, and the plus-branch solutions with $k = -1$, see Tables II and IV, respectively.

k	$\Lambda = 0$ ($-$ branch)		$\Lambda > 0$ ($-$ branch)		$\Lambda < 0$ ($-$ branch)		$+$ branch	
	$\tilde{M}$	Type	$\tilde{M}$	Type	$\tilde{M}$	Type	$\tilde{M}$	Type
1	$\tilde{M} < \tilde{M}_{\rm ex}^{(-)}$	sI	see Table II		$\tilde{M} < \tilde{M}_{\rm ex}^{(-)}$	sIV	any	sIV
	$\tilde{M} = \tilde{M}_{\rm ex}^{(-)}$	dbI			$\tilde{M} = \tilde{M}_{\rm ex}^{(-)}$	dbII		
	$\tilde{M} > \tilde{M}_{\rm ex}^{(-)}$	bVII			$\tilde{M} > \tilde{M}_{\rm ex}^{(-)}$	bIV		
0	$\tilde{M} \le 0$	sI	any	sII	$\tilde{M} < \tilde{M}_{\rm ex}^{(-)}$	sIV	any	sIV
	$\tilde{M} > 0$	sIII			$\tilde{M} = \tilde{M}_{\rm ex}^{(-)}$	dbII		
					$\tilde{M} > \tilde{M}_{\rm ex}^{(-)}$	bIV		
-1	$\tilde{M} < \tilde{M}_B$	sIII	$\tilde{M} < \tilde{M}_B$	sII	$\tilde{M} < \tilde{M}_{\rm ex}^{(-)}$	sIV	see Table IV	
	$\tilde{M} \ge \tilde{M}_B$	sVII	$\tilde{M} \ge \tilde{M}_B$	sVIII	$\tilde{M} = \tilde{M}_{\rm ex}^{(-)}$	dbII		
					$\tilde{M}_{\rm ex}^{(-)} < \tilde{M} < \tilde{M}_B$	bIV		
					$\tilde{M} \ge \tilde{M}_B$	bIII		

TABLE IV. The classification of the spacetime structures of the static solutions in the plus branch with $k = -1$ in the Einstein-Gauss-Bonnet-Maxwell-Λ system. The numbers in the column "Type" imply the types of the conformal diagrams in Figs. 6–9.

$\lvert\tilde{Q}\rvert < \lvert\tilde{Q}_d\rvert$ $(n = 6)$		$\lvert\tilde{Q}\rvert = \lvert\tilde{Q}_d\rvert$ $(n = 6)$		$\lvert\tilde{Q}\rvert > \lvert\tilde{Q}_d\rvert$ $(n = 6)$		$n = 5$	
$\tilde{M}$	Type	$\tilde{M}$	Type	$\tilde{M}$	Type	$\tilde{M}$	Type
$\tilde{M} \le \tilde{M}_B$	sIV	$\tilde{M} \le \tilde{M}_B$	sIV	$\tilde{M} \le \tilde{M}_B$	sIV	$\tilde{M} \le \tilde{M}_B$	sIV
$\tilde{M}_B < \tilde{M} < \tilde{M}_{\rm ex}^{(1+)}$	bIII	$\tilde{M}_B < \tilde{M} < \tilde{M}_d$	bIII	$\tilde{M} > \tilde{M}_B$	bIII	$\tilde{M} > \tilde{M}_B$	bIII
$\tilde{M} = \tilde{M}_{\rm ex}^{(1+)}$	dbV	$\tilde{M} = \tilde{M}_d$	dbIV				
$\tilde{M}_{\rm ex}^{(1+)} < \tilde{M} < \tilde{M}_{\rm ex}^{(2+)}$	bVI	$\tilde{M} > \tilde{M}_d$	bIII				
$\tilde{M} = \tilde{M}_{\rm ex}^{(2+)}$	dbVII						
$\tilde{M} > \tilde{M}_{\rm ex}^{(2+)}$	bIII						

globally naked singularity. For $\tilde{M} > 0$, the solution has a cosmological horizon and represents a spacetime with a globally naked singularity.

3. $k = -1$ case

In the $k = -1$ case, solutions in the plus branch can have horizons. Since the function $U(r_{\rm ex})$ has a positive maximum in the $n \ge 6$ case, there is a solution with a doubly degenerate horizon when $|\tilde{Q}| = |\tilde{Q}_d|$, which is given by Eqs. (46) and (48). This solution belongs to the plus branch since $r_d < \sqrt{2\tilde{\alpha}}$. When $|\tilde{Q}| < |\tilde{Q}_d|$, Eq. (45) has two roots, i.e., two types of degenerate horizons exist. Since the function $U(r_{\rm ex})$ becomes positive for the range $0 < r_{\rm ex} < \sqrt{\tilde{\alpha}(n-5)/(n-3)} < \sqrt{2\tilde{\alpha}}$ in this case, these extreme solutions also belong to the plus branch. The mass of these extreme solutions is denoted as $\tilde{M}_{\rm ex}^{(1+)}$ and $\tilde{M}_{\rm ex}^{(2+)}$, where $\tilde{M}_{\rm ex}^{(1+)} < \tilde{M}_{\rm ex}^{(2+)}$, respectively. On the other hand, the function $U(r_{\rm ex})$ is negative semidefinite in $n = 5$, and there is no extreme solution.

Let us first consider the solutions in the minus branch. The $\tilde{M}$-r diagrams of the minus-branch solutions are shown in Figs. 3(c) $(n = 6)$ and 4(c) $(n = 5)$. The diagrams in $n = 5$ and higher-dimensional cases are qualitatively the same. For $\tilde{M} < \tilde{M}_B$, the solution has a cosmological horizon and represents a spacetime with a globally naked singularity. For $\tilde{M} \ge \tilde{M}_B$, the solution has no horizon and represents a spacetime with a globally naked singularity. Here $\tilde{M}_B$ is positive (negative) when $|\tilde{Q}| > |\tilde{Q}_{B,0}|$ $(|\tilde{Q}| < |\tilde{Q}_{B,0}|)$, where $|\tilde{Q}_{B,0}|$ is given by Eq. (41) as

$$\tilde{Q}_{B,0}^{\,2} = \frac{(2\tilde{\alpha})^{n-3}}{n-3}. \tag{53}$$

In the $n \ge 6$ case, the $\tilde{M}$-r diagram of the plus-branch solutions is shown in Fig. 3(d). The configuration of the $\tilde{M}$-r_h curve changes qualitatively depending on the value of the charge. First we assume $|\tilde{Q}| < |\tilde{Q}_d|$. Then there are two extreme solutions. For $\tilde{M} \le \tilde{M}_B$, the solution has no horizon and represents a spacetime with a globally naked singularity. For $\tilde{M}_B < \tilde{M} < \tilde{M}_{\rm ex}^{(1+)}$, the solution has a black hole horizon and represents the black hole spacetime. Since $|\tilde{Q}_d| < |\tilde{Q}_{B,0}|$ by Eqs. (48) and (53), $\tilde{M}_B$ is negative. So, the solution with $\tilde{M}_B < \tilde{M} < 0$ represents the negative mass black hole. For $\tilde{M} = \tilde{M}_{\rm ex}^{(1+)}$, the solution has a degenerate and a black hole horizon and represents the black hole spacetime. For $\tilde{M}_{\rm ex}^{(1+)} < \tilde{M} < \tilde{M}_{\rm ex}^{(2+)}$, the solution has three horizons. Although the RN-dS black hole solution in general relativity also has three horizons, the global structure of the present solution differs from it. By our definition the outermost and the innermost horizons of the three horizons are the black hole horizon, i.e., there are two black hole horizons, and the horizon between them is the inner horizon. For an observer locating in the untrapped region between the "inner" black hole horizon, i.e., the innermost horizon, and the inner horizon, the inner horizon would be seen as if it were the cosmological horizon. For $\tilde{M} = \tilde{M}_{\rm ex}^{(2+)}$, the solution has a black hole and a degenerate black hole horizon and represents the extreme black hole spacetime. For $\tilde{M} > \tilde{M}_{\rm ex}^{(2+)}$, the solution has a black hole horizon and represents the black hole spacetime.

When $|\tilde{Q}| = |\tilde{Q}_d|$, there is a solution with a doubly degenerate horizon. For $\tilde{M} \le \tilde{M}_B$, the solution has no horizon and represents the spacetime with a globally naked singularity. For $\tilde{M}_B < \tilde{M} < \tilde{M}_d$, the solution has a black hole horizon and represents the black hole spacetime. The solution with $\tilde{M}_B < \tilde{M} < 0$ represents the negative mass black hole. For $\tilde{M} = \tilde{M}_d$, where $\tilde{M}_d$ is given by Eqs. (46) and (47), the solution has a doubly degenerate horizon. In general relativity, there is a solution with a doubly degenerate horizon as a special case of the RN-dS solution, as shown in Sec. III B. That is not a black hole solution, while the present solution in Gauss-Bonnet gravity represents the black hole spacetime with a doubly degenerate horizon. The ratio of the charge to the mass becomes

$$\frac{|\tilde{Q}_d|}{\tilde{M}_d} = \sqrt{\frac{(n-5)^2}{8(n-3)(n-4)}} < \frac{1}{\sqrt{2}}. \tag{54}$$

For $\tilde{M} > \tilde{M}_d$, the solution has a black hole horizon and represents the black hole spacetime.

When $|\tilde{Q}| > |\tilde{Q}_d|$, no extreme solution exists. For $\tilde{M} \leq \tilde{M}_B$, the solution has no horizon and represents the spacetime with a globally naked singularity. For $\tilde{M} > \tilde{M}_B$, the solution has a black hole horizon and represents the black hole spacetime. If $|\tilde{Q}_d| < |\tilde{Q}| < |\tilde{Q}_{B,0}|$, the solution with $\tilde{M}_B < \tilde{M} < 0$ represents the negative mass black hole.

In the $n = 5$ case, the $\tilde{M}$-r diagram of the plus-branch solutions is shown in Fig. 4(d). The qualitative behavior of the solutions in the minus branch is similar to that in the $n \geq 6$ case, while that in the plus branch is a little different. Since the function $U(r_{\rm ex})$ is negative semidefinite in the $n = 5$ case, there is no extreme solution. Hence, in the plus branch, for $\tilde{M} \leq \tilde{M}_B$, the solution has no horizon and represents the spacetime with a globally naked singularity. For $\tilde{M} > \tilde{M}_B$, the solution has a black hole horizon and represents the black hole spacetime. If $|\tilde{Q}| < |\tilde{Q}_{B,0}|$, the solution with $\tilde{M}_B < \tilde{M} < 0$ represents the negative mass black hole.

B. $\Lambda > 0$

1. $k = 1$ case

The solution in the plus branch has no horizon and represents a spacetime with a globally naked singularity. On the other hand all the solutions in the minus branch have horizons. The number of horizons depends on the charge and the mass.

The $\tilde{M}$-r diagrams of the minus-branch solutions are shown in Figs. 3(e) ($n = 6$) and 4(e) ($n = 5$). Since the function $U(r_{\rm ex})$ has the positive maximum, there is a solution with a doubly degenerate horizon, whose mass and charge are given by Eqs. (50) and (51), respectively. When $|\tilde{Q}| < |\tilde{Q}_d|$, two types of extreme solutions exist whose mass is $\tilde{M}_{\rm ex}^{(1-)}$ and $\tilde{M}_{\rm ex}^{(2-)}$. For $\tilde{M} < \tilde{M}_{\rm ex}^{(1-)}$, the solution has a cosmological horizon and represents a spacetime with a globally naked singularity. For $\tilde{M} = \tilde{M}_{\rm ex}^{(1-)}$, the solution has a degenerate black hole horizon and a cosmological horizon and represents the extreme black hole spacetime. For $\tilde{M}_{\rm ex}^{(1-)} < \tilde{M} < \tilde{M}_{\rm ex}^{(2-)}$, the solution has three horizons, which are inner, black hole, and cosmological horizons. The solution represents the black hole spacetime. For $\tilde{M} = \tilde{M}_{\rm ex}^{(2-)}$, the solution has an inner horizon and a degenerate horizon and represents a spacetime with a globally naked singularity. For $\tilde{M} > \tilde{M}_{\rm ex}^{(2-)}$, the solution has a cosmological horizon and represents a spacetime with a globally naked singularity.

When $|\tilde{Q}| = |\tilde{Q}_d|$, there is a solution with a doubly degenerate horizon. For $\tilde{M} \neq \tilde{M}_d$, the solution has a cosmological horizon and represents a spacetime with a globally naked singularity. For $\tilde{M} = \tilde{M}_d$, the solution has a doubly degenerate horizon and represents a spacetime with a globally naked singularity.

When $|\tilde{Q}| > |\tilde{Q}_d|$, no extreme solution exists. All the solutions have a cosmological horizon only and represent a spacetime with a globally naked singularity.

2. $k = 0$ case

Since there is no horizon for the solution in the plus branch, all the solutions represent a spacetime with a globally naked singularity.

The $\tilde{M}$-r diagrams of the minus-branch solutions are shown in Figs. 3(f) ($n = 6$) and 4(f) ($n = 5$). The function $U(r_{\rm ex})$ is negative semidefinite so that there is no extreme solution. The solution has a cosmological horizon and represents a spacetime with a globally naked singularity for any mass parameter.

3. $k = -1$ case

The $\tilde{M}$-r diagrams are shown in Figs. 3(g) ($n = 6$, minus branch), 3(h) ($n = 6$, plus branch), 4(g) ($n = 5$, minus branch), and 4(h) ($n = 5$, plus branch). The properties of the $\tilde{M}$-r_h relations are the same as those in the $\Lambda = 0$ and $k = -1$ cases qualitatively. In the minus branch, however, the structure of the infinity is different (see the conformal diagrams).

In the case of the plus branch with $\Lambda = 0$ and $k = -1$, $\tilde{M}_B$ is always less than $\tilde{M}_{\rm ex}^{(1)}$ for $|\tilde{Q}| < |\tilde{Q}_d|$ and $n \geq 6$, as seen in Sec. V A. This is also true in the present case. By the $\tilde{M}$-r_b relation (33), r_b is a monotonically decreasing function of $\tilde{M}$, and the horizon radius of the plus-branch solution is restricted as $r_h < \sqrt{2\tilde{\alpha}}$. By these facts the mass of the solution which has a horizon should be greater than $\tilde{M}_B$. As a result, $\tilde{M}_B < \tilde{M}_{\rm ex}^{(1+)}$ is obtained. This also holds in the $\Lambda < 0$ case.

Although it is difficult to show $|\tilde{Q}_d| < |\tilde{Q}_{B,0}|$ analytically, we can show $|\tilde{Q}_d| < |\tilde{Q}_{B,0}|$ by comparing Eq. (51) with Eq. (41) in the $\tilde{\alpha} \to 0$, $\tilde{\alpha} \to \infty$, and $n \to \infty$ limits. This supports the argument that this relation should hold for any $\tilde{\alpha}$ and n. Actually the numerical calculation shows $|\tilde{Q}_d| < |\tilde{Q}_{B,0}|$. This implies that the negative mass black hole solution always exists for $|\tilde{Q}| \leq |\tilde{Q}_d|$.

C. $\Lambda < 0$

1. $k = 1$ case

The solution in the plus branch has no horizon and represents a spacetime with a globally naked singularity.

The $\tilde{M}$-r diagrams of the minus-branch solutions are shown in Figs. 3(i) ($n = 6$) and 4(i) ($n = 5$). Since the function $U(r_{\rm ex})$ monotonically increases from zero to infinity, there is an extreme solution for any $\tilde{Q}$. The extreme solution has the positive mass $\tilde{M}_{\rm ex}^{(-)} > 0$ in the $n \geq 6$ case and $\tilde{M}_{\rm ex}^{(-)} > \tilde{\alpha}$ in the $n = 5$ case. For $\tilde{M} < \tilde{M}_{\rm ex}^{(-)}$, the solution has no horizon and represents a spacetime with a globally naked singularity. For $\tilde{M} = \tilde{M}_{\rm ex}^{(-)}$, the solution has a degenerate black hole horizon and represents the

extreme black hole spacetime. For $\tilde{M} > \tilde{M}_{\rm ex}^{(-)}$, the solution has an inner and a black hole horizon and represents the black hole spacetime.

2. $k = 0$ case

The solution in the plus branch has no horizon and represents a spacetime with a globally naked singularity.

The $\tilde{M}$-r diagrams of the minus-branch solutions are shown in Figs. 3(j) ($n = 6$) and 4(j) ($n = 5$). The qualitative properties of the $\tilde{M}$-r diagram are the same as those in the $k = 1$ case except that the mass of the extreme solution is limited as $\tilde{M}_{\rm ex} > 0$ in the $n = 5$ case.

3. $k = -1$ case

If $n \geq 6$ the function $U(r_{\rm ex})$ has two extrema. However, $\tilde{Q}_d^2$ becomes negative for the minus sign in Eq. (52), and eventually there is one extreme solution with a doubly degenerate horizon. The value of the charge $\tilde{Q}_d$ of the extreme solution is determined by Eq. (51), where the plus sign is chosen in Eq. (52). When $|\tilde{Q}| < |\tilde{Q}_d|$, Eq. (45) has three roots, and there are three extreme solutions. One of them has a degenerate horizon whose radius is larger than $\sqrt{2\tilde{\alpha}}$ and belongs to the minus branch. The other belong to the plus branch. When $|\tilde{Q}| = |\tilde{Q}_d|$, the degenerate horizons in the plus branch coincide and become a doubly degenerate horizon. There is an extreme solution in each branch. When $|\tilde{Q}| > |\tilde{Q}_d|$, there is one extreme solution only in the minus branch. In the $n = 5$ case, there is only one extreme solution for fixed $\tilde{Q}$ by Eq. (45). The radius of the degenerate horizon is $r_{\rm ex} > \sqrt{2\tilde{\alpha}}$, and the extreme solution belongs to the minus branch.

First let us consider the minus branch. The $\tilde{M}$-r diagrams are shown in Figs. 3(k) ($n = 6$) and 4(k) ($n = 5$). For any value of $\tilde{Q}$, there is an extreme solution with $\tilde{M} = \tilde{M}_{\rm ex}^{(-)}$. For $\tilde{M} < \tilde{M}_{\rm ex}^{(-)}$, the solution has no horizon and represents a spacetime with a globally naked singularity. For $\tilde{M} = \tilde{M}_{\rm ex}^{(-)}$, the solution has a degenerate horizon and represents the extreme black hole spacetime. For $\tilde{M}_{\rm ex}^{(-)} < \tilde{M} < \tilde{M}_B$, the solution has an inner and a black hole horizon and represents the black hole spacetime. For $\tilde{M} \geq \tilde{M}_B$, the solution has a black hole horizon and represents the black hole spacetime.

We plot the $\tilde{M}$-$r_{\rm ex}$ curve on the $\tilde{M}$-r diagrams. For a small charge value, the extreme black hole solution has negative mass [dot E in Figs. 3(k) and 4(k). As the charge becomes large, the mass of the extreme black hole solution increases and becomes zero. We denote the charge of the zero mass extreme solution $\tilde{Q}_{\rm ex,0}$. Then when $|\tilde{Q}| < |\tilde{Q}_{\rm ex,0}|$, the mass of the extreme black hole solution is negative, and the solution with $\tilde{M}_{\rm ex}^{(-)} < \tilde{M} < 0$ represents the black hole spacetime with the negative mass. When $|\tilde{Q}| = |\tilde{Q}_{\rm ex,0}|$, the extreme solution represents the zero mass black hole spacetime. When $|\tilde{Q}| > |\tilde{Q}_{\rm ex,0}|$, all the black hole solutions have the positive mass.

We have seen that several extreme solutions appear in Gauss-Bonnet gravity. However, all of them do not have zero mass except for the one in the case of $\Lambda < 0$, $k = -1$ in the plus branch. Let us examine this situation and derive the explicit form of $\tilde{Q}_{\rm ex,0}$. By the condition $\tilde{M}_{\rm ex} = 0$ (we assume $r_{\rm ex} \neq 0$), Eq. (43) gives

$$\frac{(n-2)}{(n-3)\ell^2} r_{\rm ex}^4 + k r_{\rm ex}^2 + \frac{(n-4)\tilde{\alpha}k^2}{(n-3)} = 0. \tag{55}$$

For $\Lambda = 0$,

$$r_{\rm ex}^2 = -\frac{(n-4)\tilde{\alpha}k}{n-3}, \tag{56}$$

which implies that only the $k = -1$ case can have a positive real root. However, then the $\tilde{Q}_{\rm ex,0}$ is estimated by Eq. (44) as

$$\tilde{Q}_{\rm ex,0}^{\,2} = -\frac{2 r_{\rm ex}^{2(n-2)}}{(n-4)^2\tilde{\alpha}} < 0, \tag{57}$$

which gives a contradiction so that $\tilde{Q}_{\rm ex,0}$ is not defined in the $\Lambda = 0$ case.

For $\Lambda \neq 0$, the roots of Eq. (55) are

$$r_{\rm ex}^2 = -\frac{(n-3)\ell^2}{2(n-2)}\left[k \pm |k|\sqrt{1 - \frac{4(n-2)(n-4)\tilde{\alpha}}{(n-3)^2\ell^2}}\right]. \tag{58}$$

The value inside of the square root is guaranteed to be positive definite by the condition (31). For $k = 0$ there is no positive root. Substituting Eq. (58) into Eq. (44),

$$\tilde{Q}_{\rm ex,0}^{\,2} = -\frac{2 r_{\rm ex}^{2(n-4)}(k r_{\rm ex}^2 + 2\tilde{\alpha}k^2)}{(n-2)(n-3)}. \tag{59}$$

When $k = 1$ the rhs is negative definite. Hence only in the $k = -1$ case can $\tilde{Q}_{\rm ex,0}$ be defined. Moreover for $k = -1$, Eq. (59) gives a condition

$$r_{\rm ex}|_{\tilde{M}_{\rm ex}=0} > \sqrt{2\tilde{\alpha}}, \tag{60}$$

which implies that the extreme solution with zero mass appears only in the minus branch. Substituting Eq. (58) into this condition in the $\Lambda > 0$ case, one easily finds $4\tilde{\alpha}/\ell^2 \geq 1$, which contradicts the condition (31). In the $\Lambda < 0$ case, taking the lower (minus sign) solution of Eq. (58), one finds a similar contradiction. As a result, only in the $\Lambda < 0$ and $k = -1$ cases can we define $\tilde{Q}_{\rm ex,0}$ in the minus branch by taking the upper solution of Eq. (58). Its value is

$$\tilde{Q}_{\rm ex,0}^{\,2} = \frac{2 r_{\rm ex}^{2(n-4)}(r_{\rm ex}^2 - 2\tilde{\alpha})}{(n-2)(n-3)}, \tag{61}$$

where

$$r_{\rm ex}^2 = \frac{(n-3)\ell^2}{2(n-2)}\left[1+\sqrt{1-\frac{4(n-2)(n-4)\tilde{\alpha}}{(n-3)^2\ell^2}}\right]. \quad (62)$$

Next let us move onto the plus branch. The $\tilde{M}$-r diagrams of the plus-branch solutions are shown in Figs. 3(l) ($n=6$) and 4(l) ($n=5$). The configurations of the $\tilde{M}$-r diagrams are qualitatively the same as those in the $\Lambda=0$, $k=-1$ cases, respectively.

In the $\Lambda \geq 0$ and $k=-1$ cases, $|\tilde{Q}_d| < |\tilde{Q}_{B,0}|$ holds for any case. In the $\Lambda<0$ case, however, $|\tilde{Q}_d|$ can be larger than $|\tilde{Q}_{B,0}|$. This can be seen easily as follows. In the $\alpha \to 0$ limit,

$$\tilde{Q}_{B,0}^{\,2} \sim \frac{2^{n-3}}{n-3}\tilde{\alpha}^{n-3}, \quad (63)$$

$$\tilde{Q}_{d}^{\,2} \sim \frac{2(n-5)}{(n-3)^3}\left[\frac{(n-4)(n-5)}{(n-3)^2}\right]^{n-4}\tilde{\alpha}^{n-3}. \quad (64)$$

So in this limit, $|\tilde{Q}_d| < |\tilde{Q}_{B,0}|$. On the other hand, in the $4\tilde{\alpha}/\ell^2 \to 1$ limit, $|\tilde{Q}_{B,0}| \sim 0$ and $|\tilde{Q}_d| > 0$. Hence $|\tilde{Q}_d| > |\tilde{Q}_{B,0}|$. Therefore there is a certain value of $\tilde{\alpha}$ where the $|\tilde{Q}_{B,0}|$ and $|\tilde{Q}_d|$ are equal. $|\tilde{Q}_{\rm ex,0}|$ also vanishes in the $4\tilde{\alpha}/\ell^2 \to 1$ limit. Hence for a small $\tilde{\alpha}$, there are two extreme solutions in the plus branch for small $|\tilde{Q}| < |\tilde{Q}_d|$. Simultaneously the negative mass black hole solution exists. As the charge becomes large, extreme solutions disappear while the negative mass black hole solution remains. In the large $\tilde{\alpha}$ limit, however, the negative mass black hole solutions disappear, although the extreme solutions exist. These behaviors in the space of the solutions are interesting in the context of our discussion of the evolution of the black hole.

VI. EINSTEIN-GAUSS-BONNET-MAXWELL-Λ SYSTEM: $4\tilde{\alpha}/\ell^2 = 1$ CASE

The system with $4\tilde{\alpha}/\ell^2 = 1$ is a special case, where the vacuum states of the plus and the minus branches coincide. Since we have assumed that α is positive, the cosmological constant is negative by definition. The metric function f becomes [33]

$$f = k + \frac{r^2}{2\tilde{\alpha}}\left\{1 \mp \sqrt{4\tilde{\alpha}\left[\frac{\tilde{M}}{r^{n-1}} - \frac{(n-3)\tilde{Q}^2}{2r^{2(n-2)}}\right]}\right\}. \quad (65)$$

When the radius is large a spacetime approaches adS spacetime for $r \to \infty$ with the effective curvature radius $\ell_{\rm eff} := \sqrt{2\tilde{\alpha}}$ for $k=1$.

In the charged case, a branch singularity locates at

$$r = r_b := \left[\frac{(n-3)\tilde{Q}^2}{2\tilde{M}}\right]^{1/(n-3)}. \quad (66)$$

Hence the mass must be positive in this special case. There is no negative mass black hole solution. Furthermore the r_b is independent of the Gauss-Bonnet coefficient $\tilde{\alpha}$. The Kretschmann invariant behaves as

$$\mathcal{I} = O((r-r_b)^{-3}) \quad (67)$$

around the branch singularity. Since f behaves

$$f \approx k + \frac{r_b^2}{2\tilde{\alpha}} \mp \frac{(n-3)|\tilde{Q}|}{\sqrt{2\tilde{\alpha}}r_b^{n-4}}\sqrt{\frac{r-r_b}{r_b}} \quad (68)$$

near the branch singularity, the branch singularities are timelike [Fig. 1(a)] for the solutions with $k=0,1$. For the solutions with $k=-1$, the singularity is timelike for $r_b > \sqrt{2\tilde{\alpha}}$ and spacelike [Fig. 1(d)] for $r_b < \sqrt{2\tilde{\alpha}}$. In the special case of $r_b = \sqrt{2\tilde{\alpha}}$, the singularity is spacelike in the minus branch and timelike in the plus branch.

Since the radius of a horizon is restricted to $r_h^2 < -2\tilde{\alpha}k$ ($r_h^2 > -2\tilde{\alpha}k$) for the plus (minus) branch, there are no horizons for solutions with $k=0,1$ in the plus branch. The $\tilde{M}$-r_h relation (39) becomes

$$\tilde{M} = r_h^{n-1}\left[\frac{1}{4\tilde{\alpha}}\left(1+\frac{2k\tilde{\alpha}}{r_h^2}\right)^2 + \frac{(n-3)\tilde{Q}^2}{2r_h^{2(n-2)}}\right]. \quad (69)$$

As in the $4\tilde{\alpha}/\ell^2 \neq 1$ case, a vertical point of the $\tilde{M}$-r_h curve corresponds to a degenerate horizon. From the condition $f(r_{\rm ex}) = df/dr|_{r=r_{\rm ex}} = 0$, the relations between the mass, the charge, and the radius of the degenerate horizon of the extreme solution are

$$\tilde{M} = \tilde{M}_{\rm ex} = \frac{r_{\rm ex}^{n-1}}{2\tilde{\alpha}(n-3)}\left(1+\frac{2k\tilde{\alpha}}{r_{\rm ex}^2}\right)\left[n-2+\frac{2(n-4)k\tilde{\alpha}}{r_{\rm ex}^2}\right], \quad (70)$$

$$\tilde{Q}^2 = \tilde{Q}_{\rm ex}^2 = \frac{r_{\rm ex}^{2(n-2)}}{2\tilde{\alpha}(n-3)^2}\left(1+\frac{2k\tilde{\alpha}}{r_{\rm ex}^2}\right)\left[n-1+\frac{2(n-5)k\tilde{\alpha}}{r_{\rm ex}^2}\right]. \quad (71)$$

There is one extreme solution for any value of $\tilde{Q}$ when $k=0,1$ since the rhs of Eq. (71) monotonically increases. When $k=-1$ and $n=5$, there is also one extreme solution for any value of $\tilde{Q}$. Since the radius of the degenerate horizon is restricted to $r_{\rm ex} > \sqrt{2\tilde{\alpha}}$ by Eq. (71) for the $k=-1$ and $n=5$ cases, the extreme solution belongs to the minus branch.

When $k=-1$ and $n \geq 6$, the number of extreme solutions depends on $\tilde{Q}$. There is always one extreme solution with $\tilde{M} = \tilde{M}_{\rm ex}^{(-)}$ in the minus branch. For $|\tilde{Q}| = |\tilde{Q}_d|$, where $|\tilde{Q}_d|$ is obtained by substituting $\ell^2 = 4\tilde{\alpha}$ into Eq. (51), there is an extreme solution with a doubly degenerate horizon in the plus branch. $\tilde{M}_d$ and r_d are also obtained from Eqs. (49), (50), and (52). For

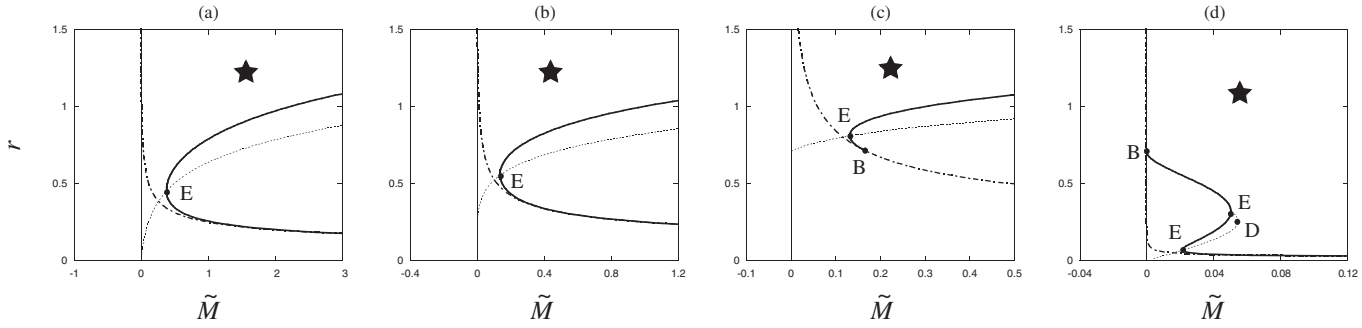

FIG. 5. The $\tilde{M}$-r diagrams of the static solutions in the six-dimensional Einstein-Gauss-Bonnet-Maxwell-Λ system with $4\tilde{\alpha}/\ell^2 = 1$. From the left-hand side, the diagrams are the $k = 1$ (the minus branch), $k = 0$ (the minus branch), $k = -1$ (the minus branch), and $k = -1$ (the plus branch) cases. We show the $\tilde{M}$-r_h relations (thick solid curves) and the $\tilde{M}$-r_b relations (dot-dashed curves). We set $\tilde{\alpha} = 0.25$ and $\tilde{Q} = 0.1$ for (a) and (b), $\tilde{Q} = 0.2$ for (c), and $\tilde{Q} = 10^{-3}$ for (d). We choose the value of the charge as $|\tilde{Q}| < |\tilde{Q}_d|$ for (d). Otherwise, the two extreme solutions in the plus branch coincide, and the $\tilde{M}$-r_h relation becomes single valued. The dotted curve represents a sequence of the degenerate horizon ($\tilde{M}$-$r_{\rm ex}$ relation) by varying $\tilde{Q}$. Below the $\tilde{M}$-r_b line or the negative mass regions, there are no solutions. See Figs. 2 and 3 for the meanings of the dots and the stars.

$|\tilde{Q}| < (>)|\tilde{Q}_d|$ there are two (no) extreme solutions with $\tilde{M}_{\rm ex}^{(1+)}$ and $\tilde{M}_{\rm ex}^{(2+)}$, where $\tilde{M}_{\rm ex}^{(1+)} < \tilde{M}_{\rm ex}^{(2+)}$, respectively, in the plus branch.

By the above analysis, we can draw the $\tilde{M}$-r diagram. The solution in the plus branch has no horizon in the $k = 1, 0$ cases and represents a spacetime with a globally naked singularity. The $\tilde{M}$-r diagrams of the minus-branch solution in the $k = 1, 0$ cases are shown in Figs. 5(a) and 5(b), respectively. The solution only exists for the positive mass parameter. Besides this fact, the properties are the same as those in the $4\tilde{\alpha} \neq \ell^2$ case [see Figs. 3(i) and 3(j)]. There is an extreme solution for any $\tilde{Q}$. For $0 < \tilde{M} < \tilde{M}_{\rm ex}^{(-)}$, the solution has no horizon and represents a spacetime with a globally naked singularity. For $\tilde{M} = \tilde{M}_{\rm ex}^{(-)}$, the solution has a degenerate black hole horizon and represents the extreme black hole spacetime. For $\tilde{M} > \tilde{M}_{\rm ex}^{(-)}$, the solution has an inner and a black hole horizon and represents the black hole spacetime.

In the $k = -1$ case, the $\tilde{M}$-r diagram of the minus-branch solution is shown in Fig. 5(c). There is an extreme solution for any $\tilde{Q}$. For $0 < \tilde{M} < \tilde{M}_{\rm ex}^{(-)}$, the solution has no horizon and represents a spacetime with a globally naked singularity. For $\tilde{M} = \tilde{M}_{\rm ex}^{(-)}$, the solution has a degenerate black hole horizon and represents the extreme black hole spacetime. For $\tilde{M}_{\rm ex}^{(-)} < \tilde{M} < \tilde{M}_B$, the solution has inner and black hole horizons and represents the black hole spacetime. For $\tilde{M}_B \leq \tilde{M}$, the solution has a black hole horizon and represents the black hole spacetime.

The $\tilde{M}$-r diagram of the plus-branch solution is shown in Fig. 5(d). The configuration of the $\tilde{M}$-r_h curve is almost the same as that in the $4\tilde{\alpha}/\ell^2 \neq 1$ case [see Fig. 3(l)] except that the mass parameter is always positive, and eventually the mass of the branch point is positive.

The spacetime structures of these solutions are summarized in Tables IV and V.

TABLE V. The classification of the spacetime structures of the static solutions in the Einstein-Gauss-Bonnet-Maxwell-Λ system with $4\tilde{\alpha}/\ell^2 = 1$. The numbers in the column "Type" imply the types of the Penrose diagrams drawn in Figs. 6–9. For the plus-branch solution with $k = -1$, see Table IV, where the range $\tilde{M} \leq \tilde{M}_B$ should be changed to $0 < \tilde{M} \leq \tilde{M}_B$.

k	− branch		+ branch	
	$\tilde{M}$	Type	$\tilde{M}$	Type
1, 0	$0 < \tilde{M} < \tilde{M}_{\rm ex}^{(-)}$	sIV	$\tilde{M} > 0$	sIV
	$\tilde{M} = \tilde{M}_{\rm ex}^{(-)}$	dbII		
	$\tilde{M} > \tilde{M}_{\rm ex}^{(-)}$	bIV		
-1	$0 < \tilde{M} < \tilde{M}_{\rm ex}^{(-)}$	sIV	see Table IV	
	$\tilde{M} = \tilde{M}_{\rm ex}^{(-)}$	dbII	(The range $\tilde{M} \leq \tilde{M}_B$ is	
	$\tilde{M}_{\rm ex}^{(-)} < \tilde{M} < \tilde{M}_B$	bIV	changed to $0 < \tilde{M} \leq \tilde{M}_B$.)	
	$\tilde{M} \geq \tilde{M}_B$	bIII		

VII. CONCLUSIONS AND DISCUSSION

We have studied spacetime structures of the static solutions in the n-dimensional Einstein-Gauss-Bonnet-Maxwell-Λ system, where the cosmological constant is either positive, zero, or negative. We assume that the Gauss-Bonnet coefficient α is non-negative. This assumption is consistent with the notion that the action is derived from superstring/M theory in the low-energy limit. The solutions have the $(n-2)$-dimensional Euclidean submanifold whose curvature is $k = 1, 0$, or -1. We assume $4\tilde{\alpha}/\ell^2 \leq 1$ in order to define the relevant vacuum state. The structures of the center, horizons, infinity, and the singular point depend on the parameters of the system and the branches complicatedly so that a variety of global structures for the solution is found. In our analysis, the

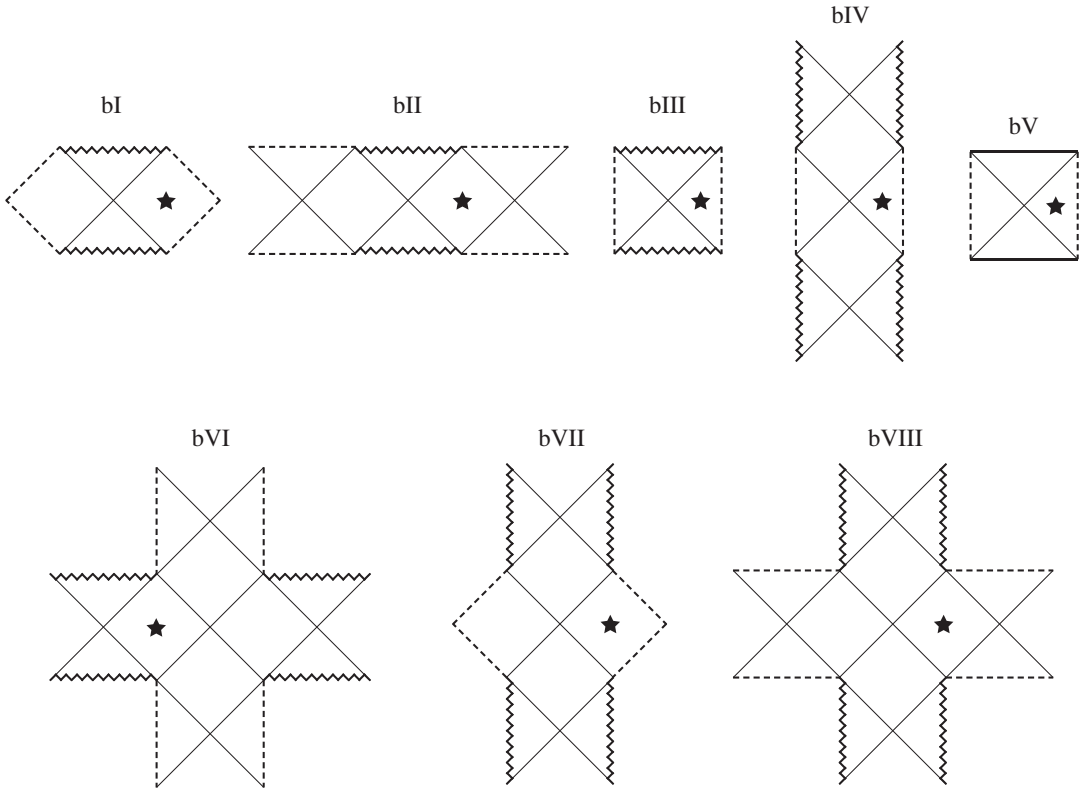

FIG. 6. The conformal diagrams of black hole solutions. bI, bII, bIII, bIV, bVII, and bVIII have the same structure as those of the Schwarzschild, Schwarzschild-dS, Schwarzschild-adS, RN-adS, RN, and RN-dS spacetimes, respectively.

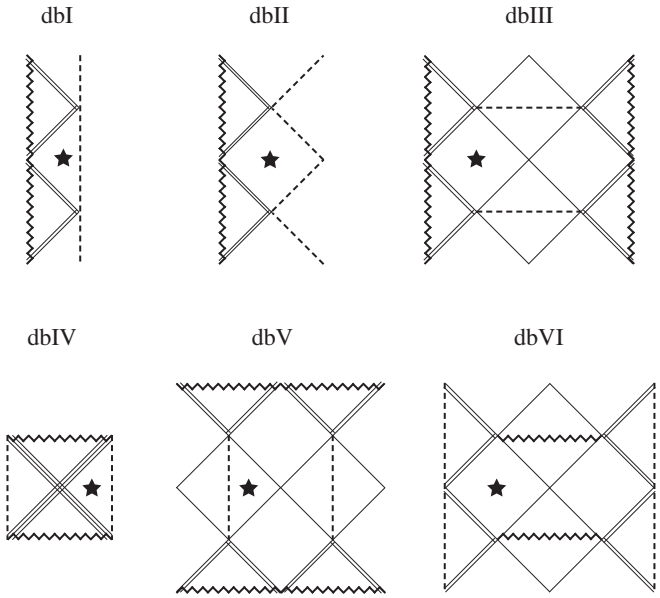

FIG. 7. The conformal diagrams of black hole solutions with degenerate horizons. The degenerate horizon is drawn with a double or triple line according to its degeneracy. By passing across the triple (double) line, the trapped region (does not) changes to an untrapped one. dbI, dbII, and dbIII have the same structure as those of the extreme RN-adS, extreme RN, and extreme RN-dS spacetimes with degenerated horizons of the inner and black hole horizons, respectively. dbIV is the case with triple degenerate horizons. Although the horizontal lines in dbIII are the infinities, they show distinct infinities by a single line depending on how to approach (from above or from below) them.

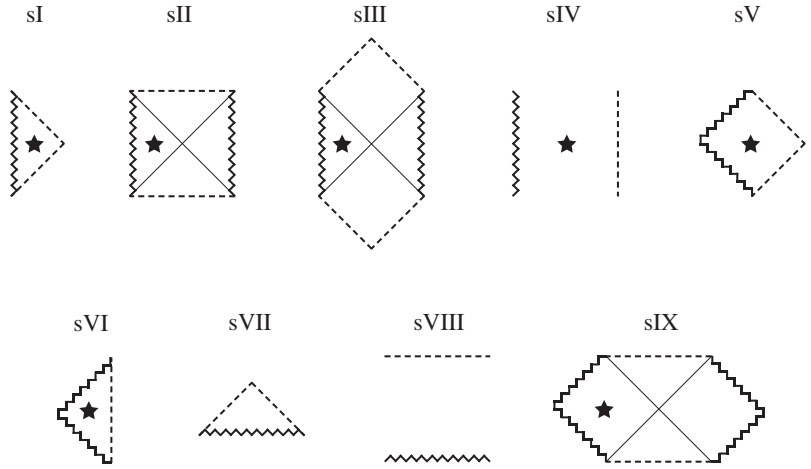

FIG. 8. The conformal diagrams of the solutions with a globally naked singularity. There are time-reversed diagrams for sVII and sVIII.

$\tilde{M}$-r diagram provides an easily understood visual classification.

In Gauss-Bonnet gravity, the solutions are classified into plus and minus branches. In the $\tilde{\alpha} \to 0$ limit, the solution in the minus branch recovers the one in general relativity, while there is no solution in the plus branch. The structure of the infinity is not determined by the cosmological constant alone but also by the effective curvature radius $\ell_{\rm eff}^2$. In the minus branch the ordinary correspondence between the signs of the cosmological constant Λ and the asymptotic structures is obtained. In the plus branch, however, the sign of $\ell_{\rm eff}^2$ is always positive independent of the cosmological constant, so that all the solutions have the same asymptotic structure as those in general relativity with a negative cosmological constant.

In general relativity, when one adds a charge to the Schwarzschild black hole, the inner horizon appears, and the singularity changes from spacelike to timelike. Also in Gauss-Bonnet gravity, the charge affects greatly the central region of a spacetime. In the charged solutions a singularity appears at the finite radius $r = r_b > 0$, which is called a branch singularity. Although in the neutral case the branch singularity appears only for the negative mass parameter, in the charged case it appears for any mass parameter. It becomes timelike or spacelike depending on the parameters. Furthermore, the Kretschmann invariant behaves as $O((r - r_b)^{-3})$ around the branch singularity. This is much milder than divergent behavior of the central singularity in general relativity $O(r^{-4(n-2)})$. This may imply that the string effects make the singular behavior milder.

There are three types of horizons: inner, black hole, and cosmological horizons. In the $k = 1, 0$ cases the plus-branch solutions do not have any horizon. In the $k = -1$ case, the radius of the horizon is restricted as $r_h < \sqrt{2\tilde{\alpha}}$ ($r_h > \sqrt{2\tilde{\alpha}}$) in the plus (minus) branch. The point with $r_h = \sqrt{2\tilde{\alpha}}$ on the $\tilde{M}$-r_h relation is the branch point whose mass is $\tilde{M}_B$. In the neutral case $\tilde{M}_B$ is always negative, so that there is a black hole solution with negative mass. However, in the charged case $\tilde{M}_B$ becomes zero when $|\tilde{Q}| = |\tilde{Q}_{B,0}|$, and $\tilde{M}_B > 0$ for $|\tilde{Q}| > |\tilde{Q}_{B,0}|$.

Among the solutions in our analysis, the black hole solutions would be the most important. Although the $\tilde{M}$-r_h relations in the $k = 1, 0$ cases have qualitatively similar configurations to those in general relativity, the solution in the $k = -1$ case is quite different. The charged

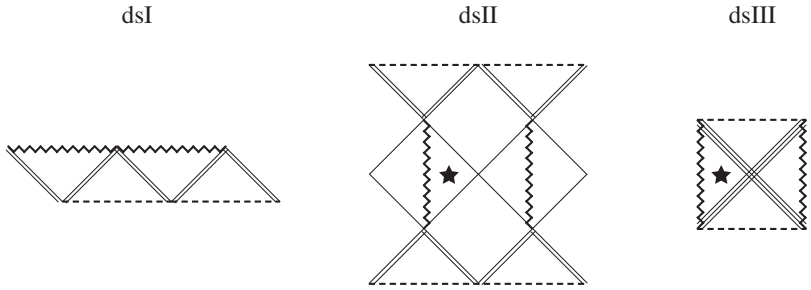

FIG. 9. The conformal diagrams of the solutions with a globally naked singularity and degenerate horizons. The timelike singularities in dsII show distinct singularities by a single wavy line depending on how to approach (from the right- or left-hand side) to them. There is a time-reversed diagram for dsI.

black hole solution in general relativity always has an inner horizon, and the singularity is timelike. For the $k = 1$ and 0 cases in Gauss-Bonnet gravity, the singularity of the black hole solution is timelike, too. Most of the black hole solutions with $k = -1$, however, have no inner horizon so that the branch singularity of these solutions becomes spacelike. When $|\tilde{Q}| < |\tilde{Q}_{B,0}|$, there are black hole solutions with zero and negative mass in the plus branch for $k = -1$ regardless of the sign of the cosmological constant. Although there is maximum mass for the black hole solutions in the plus branch for $k = -1$ in the neutral case, no such maximum exists in the charged case, and any positive mass solution is black hole for $|\tilde{Q}| < |\tilde{Q}_{B,0}|$. A solution has three horizons at most. In general relativity, the RN-dS black hole solution has three horizons which are the inner, the black hole, and the cosmological horizons. In Gauss-Bonnet gravity, the solutions in the plus branch with $k = -1$ and $n \geq 6$ have three horizons for each cosmological constant when $|\tilde{Q}| < |\tilde{Q}_d|$ and $\tilde{M}_{\rm ex}^{(1+)} < \tilde{M} < \tilde{M}_{\rm ex}^{(2+)}$. The horizons of these solutions are the inner black hole, the inner, and the ''outer'' black hole horizons. We add the words inner and outer to distinguish each black hole horizon.

We investigate the system with the special parameter $4\tilde{\alpha}/\ell^2 = 1$ separately where the vacuum states in the plus and minus branches coincide. In this case only is the positive mass solution allowed; otherwise the metric function takes a complex value.

Considering the Gauss-Bonnet effects on the CCH, we find first that the divergent behavior around the singularity becomes milder than that in general relativity. It is, however, difficult to eliminate the singularity completely. Second, most of the black hole solutions in the $k = -1$ case have no inner horizon, and the singularity is spacelike. However, all the black hole solutions in the $k = 1$ and 0 cases still have the timelike singularity. Furthermore since the structure of the infinity of the black hole solution with $k = -1$ is adS-like, the spacetime is not globally hyperbolic. As a result, the Gauss-Bonnet terms do not work quite as well from the cosmic censorship spirit.

Let us consider the evolution of the black hole solutions. In the RN-dS black hole spacetime in general relativity, the spacetime seems to evolve to the one with globally naked singularity by throwing some mass into the black hole such that the mass of the black hole becomes larger than that of the extreme black hole solution $\tilde{M}_{\rm ex}^{(2)}$. However, it will not happen as discussed in Ref. [35]. In Gauss-Bonnet gravity, the situation is quite different. In the nonextreme neutral black hole spacetime in the plus branch with $k = -1$, there are inner and black hole horizons without a cosmological horizon [9]. When one puts the mass into the black hole, the radius of the black hole decreases [36]. If more matter is added, the black hole may evolve to the extreme black hole with finite processes and then to a spacetime with a globally naked singularity. This is a classical transition from the black hole spacetime to the one with a globally naked singularity. Next let us consider the charged case where the black hole spacetime has the inner black hole, and the inner and the outer black hole horizons. This solution exists in the plus branch for $n \geq 6$. Adding the mass to the black hole, the black hole approaches the extreme solution, and then it transits to the black hole spacetime with a smaller horizon whose mass is $\tilde{M} > \tilde{M}_{\rm ex}^{(2+)}$. This is a classical transition from one black hole spacetime to another black hole spacetime. On the other hand, another process, i.e., the Hawking evaporation process, may occur in our black hole spacetime. The black hole in this plus-branch solution may evaporate and lose its mass. Then, what happens when the mass of the black hole becomes $\tilde{M} = \tilde{M}_{\rm ex}^{(1+)}$, where the horizon inside of the outer black hole horizon degenerates? To obtain the precise scenario of the evolutions of black hole spacetime through classical and quantum processes, we need a detailed analysis.

There are some applications and extensions of the present investigation. We find that the static solutions in Gauss-Bonnet gravity have much variety and interesting properties. One of the most important issues is stability of the solutions. There are some studies which support the dynamical stability of the exterior spacetime of the black hole solutions in Gauss-Bonnet gravity [37–39]. However, they do not cover all the cases, and there remain some unclear analyses. The problem of the stability of the inner horizons has also been raised. This is interesting from the CCH point of view [40,41]. We find several solutions with degenerate horizons. They correspond to the solutions with the product metric such as the Nariai and the Bertotti-Robinson solutions. All the solutions of this type in the Einstein-Maxwell-Λ system have been recently classified in Ref. [42]. It would be interesting to extend the analysis to Gauss-Bonnet gravity. Another application is to the braneworld. The solution with a negative cosmological constant and/or in the plus branch has the adS-like structure of the infinity. These solutions can be applied to the bulk spacetime of the braneworld and are currently under investigation.

ACKNOWLEDGMENTS

We would like to thank Kei-ichi Maeda, Umpei Miyamoto, and Masato Nozawa for discussions. This work was partially supported by a Grant for The 21st Century COE Program (Holistic Research and Education Center for Physics Self-Organization Systems) at Waseda University.

[1] N. Arkani-Hamed, S. Dimopoulos, and G. Dvali, Phys. Lett. B **429**, 263 (1998); I. Antoniadis, N. Arkani-Hamed, S. Dimopoulos, and G. Dvali, Phys. Lett. B **436**, 257 (1998).

[2] L. Randall and R. Sundrum, Phys. Rev. Lett. **83**, 3370 (1999); **83**, 4690 (1999).

[3] G. Dvali, G. Gabadadze, and M. Porrati, Phys. Lett. B **485**, 208 (2000); G. Dvali and G. Gabadadze, Phys. Rev. D **63**, 065007 (2001); G. Dvali, G. Gabadadze, and M. Shifman, Phys. Rev. D **67**, 044020 (2003).

[4] S. Dimopoulos and G. Landsberg, Phys. Rev. Lett. **87**, 161602 (2001); A. Chamblin and G. C. Nayak, Phys. Rev. D **66**, 091901 (2002); S. B. Giddings and S. Thomas, Phys. Rev. D **65**, 056010 (2002).

[5] P. Hořava and E. Witten, Nucl. Phys. **B475**, 94 (1996); A. Lukas, B. A. Ovrut, K. S. Stelle, and D. Waldram, Phys. Rev. D **59**, 086001 (1999); A. Lukas, B. A. Ovrut, and D. Waldram, Phys. Rev. D **60**, 086001 (1999).

[6] D. J. Gross and E. Witten, Nucl. Phys. **B277**, 1 (1986); D. J. Gross and J. H. Sloan, Nucl. Phys. **B291**, 41 (1987); R. R. Metsaev and A. A. Tseytlin, Phys. Lett. B **191**, 354 (1987); R. C. Meyers, Phys. Rev. D **36**, 392 (1987); C. G. Callan, R. C. Myers, and M. J. Perry, Nucl. Phys. **B311**, 673 (1989); R. R. Metsaev and A. A. Tseytlin, Nucl. Phys. **B293**, 385 (1987).

[7] B. Zwieback, Phys. Lett. **156B**, 315 (1985); B. Zumino, Phys. Rep. **137**, 109 (1986).

[8] Y. Choquet-Bruhat, C. R. Acad. Sci. I, Math **306**, 445 (1988); J. Math. Phys. (N.Y.) **29**, 1891 (1988).

[9] T. Torii and H. Maeda, Phys. Rev. D **71**, 124002 (2005).

[10] D. G. Boulware and S. Deser, Phys. Rev. Lett. **55**, 2656 (1985).

[11] J. T. Wheeler, Nucl. Phys. **B268**, 737 (1986).

[12] See, for example, T. Torii, H. Yajima, and K. Maeda, Phys. Rev. D **55**, 739 (1997), and references therein.

[13] D. Lovelock, J. Math. Phys. (N.Y.) **12**, 498 (1971); **13**, 874 (1972).

[14] J. T. Wheeler, Nucl. Phys. **B273**, 732 (1986).

[15] R. C. Myers and J. Z. Simon, Phys. Rev. D **38**, 2434 (1988). The black hole solution in Gauss-Bonnet gravity is explicitly provided, and the charged solution is also briefly discussed.

[16] B. Whitt, Phys. Rev. D **38**, 3000 (1988).

[17] R. Penrose, Riv. Nuovo Cimento **1**, 252 (1969).

[18] R. Penrose, in *General Relativity, an Einstein Centenary Survey*, edited by S. W. Hawking and W. Israel (Cambridge University Press, Cambridge, UK, 1979), p. 581.

[19] R. Penrose, in *Battelle Rencontres*, edited by C. de Witt and J. A. Wheeler (W. A. Benjamin, New York, 1968), p. 222.

[20] E. Poisson and W. Israel, Phys. Rev. D **41**, 1796 (1990).

[21] P. R. Brady, Prog. Theor. Phys. Suppl. **136**, 29 (1999).

[22] T. Harada, Pramana **63(4)**, 741 (2004).

[23] J. M. Maldacena, Adv. Theor. Math. Phys. **2**, 231 (1998); E. Witten, Adv. Theor. Math. Phys. **2**, 253 (1998); S. Gubser, I. Klebanov, and A. Polyakov, Phys. Lett. B **428**, 105 (1998); O. Aharony, S. Gubser, J. Maldacena, H. Ooguri, and Y. Oz, Phys. Rep. **323**, 183 (2000).

[24] C. Csáki, J. Erlich, and C. Grojean, Nucl. Phys. **B604**, 312 (2001).

[25] C. W. Misner, K. S. Thorne, and J. A. Wheeler, *Gravitation* (Freeman, San Francisco, 1973).

[26] The $k = 1$ case is discussed in D. L. Wiltshire, Phys. Lett. **169B**, 36 (1986).

[27] H. Kodama and A. Ishibashi, Prog. Theor. Phys. **111**, 29 (2004); gr-qc/0312012.

[28] In the higher-dimensional cases, the $(n-2)$-dimensional Einstein space is not necessarily sphere or its quotient space even for positive curvature. Hence the solution represents not only the (at least locally) RN spacetime but also many others. However, we refer to all such cases together as ''RN spacetimes.'' In the following sections we will also follow this usage.

[29] J. D. Brown, J. Creighton, and R. B. Mann, Phys. Rev. D **50**, 6394 (1994).

[30] See references in R.-G. Cai and K.-S. Soh, Phys. Rev. D **59**, 044013 (1999).

[31] M. Cvetic, S. Nojiri, and S. Odintos, Nucl. Phys. **B628**, 295 (2002).

[32] M. H. Dehghani, Phys. Rev. D **70**, 064019 (2004).

[33] In Ref. [34], the black hole solutions in Lovelock gravity with some special combination of the Lovelock coefficients are studied. Our solutions in this section coincide with those in Ref. [34].

[34] M. Bañados, C. Teitelboim, and J. Zenelli, Phys. Rev. D **49**, 975 (1994); R.-G. Cai and K.-S. Soh, Phys. Rev. D **59**, 044013 (1999); R. Aros, R. Troncoso, and J. Zenelli Phys. Rev. D **63**, 084015 (2001).

[35] T. Chiba, K. Maeda, K. Nakao, and T. Tsukamoto Phys. Rev. D **57**, 6119 (1998).

[36] Since entropy of the black hole increases, the decrease of the area of the black hole horizons does not contradict the second law of black hole thermodynamics.

[37] I. P. Neupane, Phys. Rev. D **69**, 084011 (2004).

[38] G. Dotti and R. J. Gleiser, Classical Quantum Gravity **22**, L1 (2005).

[39] T. Konoplya, Phys. Rev. D **71**, 024038 (2005).

[40] R. Penrose, in *Battelle Rencontres*, edited by C. de Witt and J. A. Wheeler (W. A. Benjamin, New York, 1968), p. 222; E. Poisson and W. Israel, Phys. Rev. D **41**, 1796 (1990); P. R. Brady, Prog. Theor. Phys. Suppl. **136**, 29 (1999).

[41] See also the references in H. Maeda, T. Torii, and T. Harada, Phys. Rev. D **71**, 064015 (2005).

[42] V. Cardoso, Ó. J. C. Dias, and J. P. S. Lemos, Phys. Rev. D **70**, 024002 (2004).